Time-resolved FRET between GPCR ligands reveals oligomers in native tissues

Laura Albizu[1-3,12,13], Martin Cottet[1-3,12], Michaela Kralikova[4-6,14], Stoytcho Stoev[7], René Seyer[1-3], Isabelle Brabet[1-3], Thomas Roux[8], Hervé Bazin[8], Emmanuel Bourrier[8], Laurent Lamarque[8], Christophe Breton[9], Marie-Laure Rives[4-6], Amy Newman[10], Jonathan Javitch[4-6,11], Eric Trinquet[8], Maurice Manning[7], Jean-Philippe Pin[1-3*], Bernard Mouillac[1-3*], Thierry Durroux[1-3*]

[1]CNRS, UMR 5203, Institut de Génomique Fonctionnelle, Montpellier, France
[2]INSERM, U. 661, Montpellier, France
[3]Université Montpellier 1and 2, Montpellier, France.

[4]Center for Molecular Recognition and [5]Department of Psychiatry, Columbia University College of Physicians and Surgeons, New York, New York, USA.
[6]Division of Molecular Therapeutics, New York State Psychiatric Institute, New York, New York, USA.

[7]Department of Biochemistry and Cancer Biology, University of Toledo College of Medicine, Toledo, USA.

[8]Cisbio Bioassays, Bagnols sur Cèze, France.

[9]Laboratoire de Neuroendocrinologie du Développement, Département de Physiologie, UPRES-EA 2701, Université des Sciences et Technologies de Lille, Villeneuve d'Ascq, France.

[10] Medicinal Chemistry Section, National Institute on Drug Abuse, Intramural Research Program, National Institutes of Health, Baltimore, Maryland, USA

[11]Department of Pharmacology, Columbia University College of Physicians and Surgeons, New York, New York, USA.

[12]Contributed equally to this work

[13]Present address: Department of Neurology, Sealfon laboratory, Mount Sinai School of Medicine, New York, NY 10029, USA

[14]Present address: Department of Auditory Neuroscience, Czech Academy of Science, Czech Republic.

[*]Corresponding authors.
Address : Institut de Génomique Fonctionnelle, CNRS UMR 5203, INSERM U. 661, 141 rue de la Cardonille 34094 Montpellier Cedex 5, France
E-mail address: tdurroux@igf.cnrs.fr
E-mail address: jppin@igf.cnrs.fr
E-mail address: bmouillac@igf.cnrs.fr
Phone: (33) 467 142 916

Nature Chemical Biology: doi: 10.1038/nchembio.396

Table of content

Nature Chemical Biology: doi: 10.1038/nchembio.396

- **Supplementary Figure 20**: absorbance spectrum of HO-[Thr^4,Orn^8(Eu-PBBP)]VT (**5**).
- **Supplementary Figure 21**: Mass spectra of HO-[Thr^4,Orn^8 (Eu-PBBP)]VT (**5**).
- **Supplementary Figure 22**: absorbance spectrum of [Lys^8(Eu-PBBP)]PVA (**1**).
- **Supplementary Figure 23**: HPLC spectrum of HO-[Thr^4, Orn^8(Alexa 647)]VT (**6**).
- **Supplementary Figure 24**: absorbance spectrum of HO-[Thr^4, Orn^8(Alexa 647)]VT (**6**).
- **Supplementary Figure 25**: mass spectrum of HO-[Thr^4, Orn^8(Alexa 647)]VT (**6**) .
- **Supplementary Figure 26**: HPLC spectrum of [Lys^8(Alexa 647)]PVA (**2**).
- **Supplementary Figure 27**: mass spectrum of [Lys^8(Alexa 647)]PVA (**2**).
- **Supplementary Figure 28**: HPLC spectrum of [Lys^8(Lumi4-Tb)]PVA (**13**) .
- **Supplementary Figure 29**: absorbance spectrum of [Lys^8(Lumi4-Tb)]PVA (**13**).
- **Supplementary Figure 30**: Mass spectrum of [Lys^8(Lumi4-Tb)]PVA (13).
- **Supplementary Figure 31**: HPLC spectrum of d$(CH_2)_5$[DTyr(Et)^2, Ile^4, Eda(Lumi4-Tb)^9]VP (**3**).
- **Supplementary Figure 32**: Absorbance spectrum of d$(CH_2)_5$[DTyr(Et)^2, Ile^4, Eda(Lumi4-Tb)^9]VP (**3**).
- **Supplementary Figure 33**: Mass spectrometry characterization of d$(CH_2)_5$[DTyr(Et)^2, Ile^4, Eda(Lumi4-Tb)^9]VP (**3**).
- **Supplementary Figure 34**: HPLC spectrum of d$(CH_2)_5$[DTyr(Et)^2, Ile^4, Eda(Alexa 488)^9]VP (**4**).
- **Supplementary Figure 35**: Absorbance spectrum of d$(CH_2)_5$[DTyr(Et)^2, Ile^4, Eda(Alexa 488)^9]VP (**4**).
- **Supplementary Figure 36**: Mass spectrometry characterization of d$(CH_2)_5$[DTyr(Et)^2, Ile^4, Eda(Alexa 488)^9]VP (**4**).
- **Supplementary Figure 37**: Mass spectrometry characterization of NAPS-NH2 (**7**).
- **Supplementary Figure 38**: 1H NMR spectrum of NAPS-NH_2 (**7**).
- **Supplementary Figure 39**: 13C NMR spectrum of NAPS-NH_2 (**7**).
- **Supplementary Figure 40**: Mass spectrum of NAPS-Glu-CO_2H.
- **Supplementary Figure 41**: 1H NMR of NAPS-Glu-CO_2H.
- **Supplementary Figure 42**: 13C NMR of NAPS-Glu-CO_2H.
- **Supplementary Figure 43**: HPLC spectrum of NAPS(Lumi4-Tb) (**8**).

Nature Chemical Biology: doi: 10.1038/nchembio.396

- **Supplementary Figure 44**: Absorbance spectrum of NAPS(Lumi4-Tb) (**8**).
- **Supplementary Figure 45**: Mass spectrometry characterization of NAPS(Lumi4-Tb) (**8**).
- **Supplementary Figure 46**: HPLC spectrum of NAPS(d1) (**9**).
- **Supplementary Figure 47**: Absorbance spectrum of NAPS(d1) (**9**).
- **Supplementary Figure 48**: Mass spectrometry characterization of NAPS(d1) (**9**).
- **Supplementary Figure 49**: Mass spectrometry characterization of PPHT-NH_2 (**10**).
- **Supplementary Figure 50**: 1H NMR of PPHT-NH_2 (**10**).
- **Supplementary Figure 51**: 13C NMR of PPHT-NH_2 (**10**).
- **Supplementary Figure 52**: Mass spectrometry characterization of PPHT-Glu-CO_2H.
- **Supplementary Figure 53**: 1H NMR of PPHT-Glu-CO_2H.
- **Supplementary Figure 54**: 13C NMR of PPHT-Glu-CO_2H.
- **Supplementary Figure 55**: HPLC spectrum of PPHT(Lumi4-Tb) (**11**).
- **Supplementary Figure 56**: Absorbance spectrum of PPHT(Lumi4-Tb) (**11**).
- **Supplementary Figure 57**: Mass spectrometry characterization of PPHT(lumi4-Tb) (**11).**
- **Supplementary Figure 58**: HPLC spectrum of PPHT(d1) (**12**).
- **Supplementary Figure 59**: Absorbance spectrum of PPHT(d1) (**12**).
- **Supplementary Figure 60**: Mass spectrometry characterization of PPHT(d1) (**12**).

3°) Additional references

Nature Chemical Biology: doi: 10.1038/nchembio.396

Supplementary Results

Supplementary Table 1: Pharmacological properties of fluorescent antagonists and agonists for the V_{1a} and oxytocin receptors.

Ligand	Affinity (K_i, nM)			Activity	
	h–V_{1a}	h-OTR	r-OTR	K_{act} (nM)	K_{inact} (nM)
[Lys^8(Eu-PBBP)]PVA	1.54 ± 0.65*	0.64 ± 0.1*	3.8 ± 0.69	nd	2.7 ± 1.1*
[Lys^8(Lumi4-Tb)]PVA	Nd	0.11 ± 0.04	0.18 ± 0.03	nd	nd
[Lys^8(Alexa 647)]PVA	3.6 ± 2*	1.91 ± 0.67*	2.68 ± 0.5	nd	0.66 ± 0.28*
HO-(Thr^4,Orn^8(Eu-PBBP)]VT	Nd	0.78 ± 0.1	0.54 ± 0.027	5.53 ± 1.27	nd
HO-(Thr^4,Orn^8(Alexa 647)]VT	Nd	0.54 ± 0.14	0.26 ± 0.015	50 ± 10	nd

The inhibition constants (K_i) of the ligands were determined by radioactive competition binding assays performed on membrane preparations of CHO cells expressing human V_{1a} (h-V_{1a}) and oxytocin (h-OTR) receptors or of lactating rat mammary glands (r-OTR). The activation constant (K_{act}) of the agonists were measured by radioactive inositol phosphate assays on CHO cells expressing oxytocin receptors. All the values are the mean ± SEM of three separate experiments performed in triplicate. *: values from [1]. nd: not determined.

Supplementary Table 2: Affinity of the fluorescent antagonists for the vasopressin V_2 receptor

Ligand	K_i (nM)
d$(CH_2)_5$[DTyr(Et)^2, Ile^4, Eda(Lumi4-Tb)^9]VP	3.2 ± 1.7
d$(CH_2)_5$[DTyr(Et)^2, Ile^4, Eda(Alexa 488)^9]VP	2.8 ± 1

The inhibition constants (K_i) of the ligands were determined by radioactive competition binding assays performed on membrane preparations of CHO cells expressing human V_2 receptors. All the values are the mean ± SEM of three separate experiments performed in triplicate.

Nature Chemical Biology: doi: 10.1038/nchembio.396

Supplementary Table 3: Affinity of the fluorescent antagonists and agonists for the dopamine D_2 receptor

Ligand	K_d (nM)
NAPS(Lumi4-Tb)	1.57 ± 0.02
NAPS(d1)	4.4 ± 0.9
PPHT(Lumi4-Tb)	8.0 ± 0.2
PPHT(d1)	9.1 ± 0.9

The dissociation constants (K_d) of the ligands were determined by saturation binding assays performed on Cos7 cells expressing human dopamine D_2 receptors. All the values are the mean ± SEM of three separate experiments performed in triplicate.

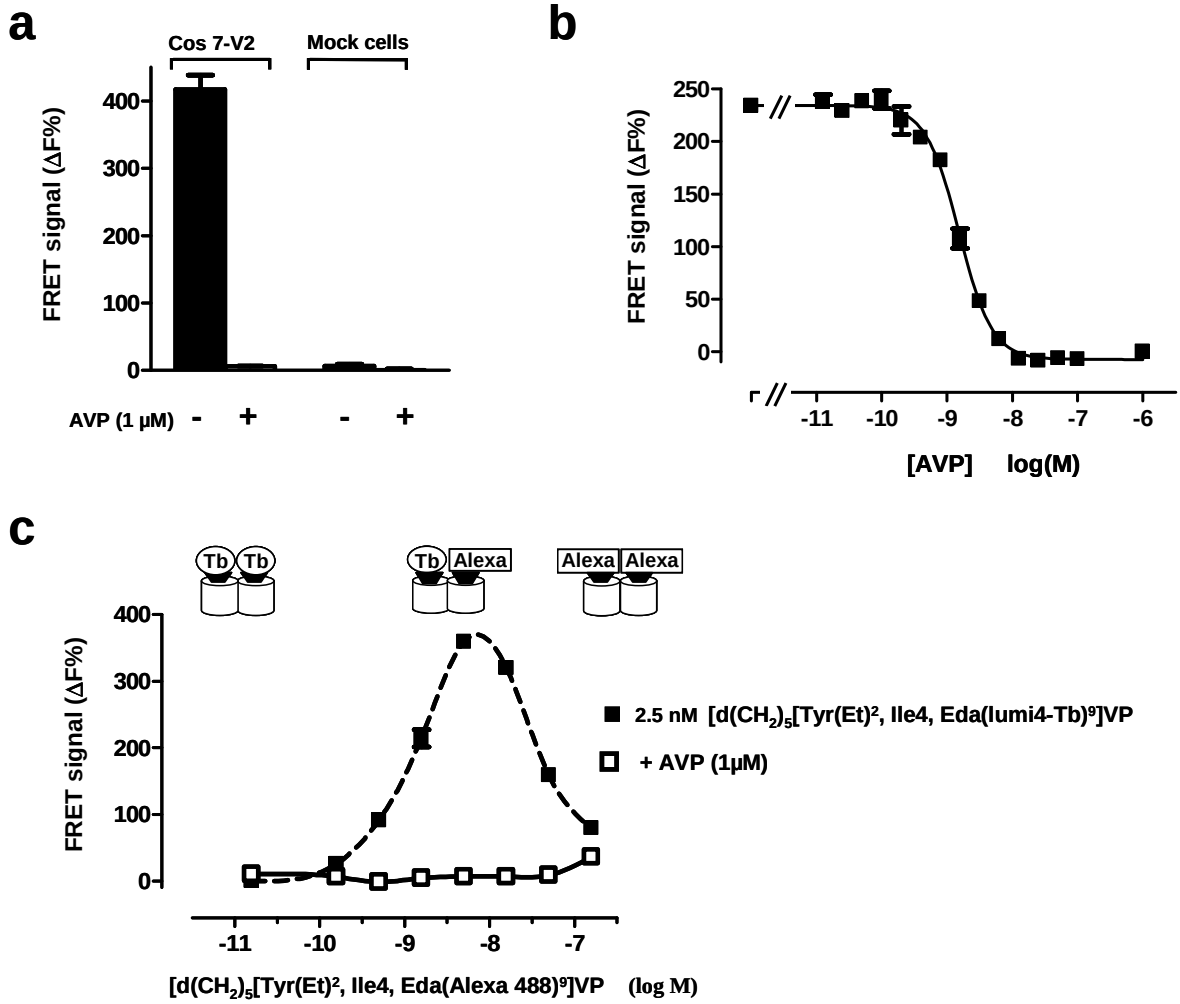

Supplementary Figure 1: FRET on V_2 receptor

a, FRET signal observed on Cos7 cells transiently transfected with V_2 receptors or on mock cells and labeled with $d(CH_2)_5[DTyr(Et)^2, Ile^4, Eda(Lumi4\text{-}Tb)^9]VP$ (**3**) (2.3 nM) and

Nature Chemical Biology: doi: 10.1038/nchembio.396

$d(CH_2)_5$[DTyr(Et)^2, Ile^4, Eda(Alexa 488)^9]VP (**4**) (4.5 nM) in the absence or presence of an excess of AVP (1µM). **b**, Inhibition of the FRET signal by increasing concentrations of AVP. Cells were incubated in the presence of $d(CH_2)_5$[DTyr(Et)^2, Ile^4, Eda(Lumi4-Tb)^9]VP (2.3 nM), $d(CH_2)_5$[DTyr(Et)^2, Ile^4, Eda(Alexa 488)^9]VP (4.5 nM) and increasing concentration of AVP. The best fit of the curve leads to an IC_{50}= 1.53 nM which is in good relation with the known affinity of vasopressin (1.8 $\pm$ 0.7 nM) [2]. **c**, Variations in the FRET signal on V_2 receptor-expressing Cos7 cells as a function of ligand concentration. Cells were incubated in the presence of 2.5 nM of $d(CH_2)_5$[DTyr(Et)^2, Ile^4, Eda(Lumi4-Tb)^9]VP and increasing concentration of $d(CH_2)_5$[DTyr(Et)^2, Ile^4, Eda(Alexa 488)^9]VP.

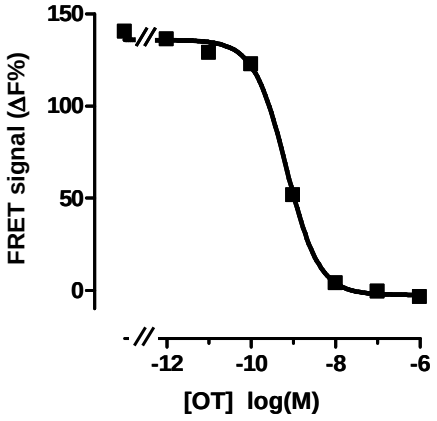

Supplementary Figure 2: **Competition binding experiments on mammary gland membrane preparation of lactating rate.** Membrane were incubated overnight at 4°C with [Lys^8(Eu-PBBP)]PVA (**1**) (1 nM), [Lys^8(Alexa 647)]PVA (**2**) (1 nM) and increasing concentrations of oxytocin. The inhibition by oxytocin led to an IC_{50} (0.46 $\pm$ 0.1 nM) corresponding to its known affinity [3]

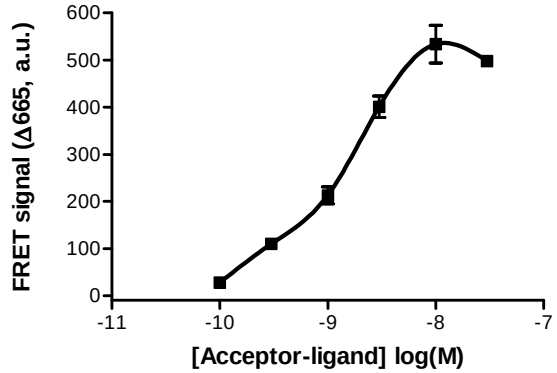

Supplementary Figure 3: [Lys^8(Lumi4-Tb)]PVA (13) is compatible with ([Lys^8(Alexa 647)]PVA (2)) to generate a FRET signal. Mammary gland membranes prepared from lactating rate were incubated overnight at 4°C in the presence of [Lys^8(Lumi4-Tb)]PVA (**13**) (0.35nM) and increasing concentrations of [Lys^8(Alexa 647)]PVA (**2**).

Nature Chemical Biology: doi: 10.1038/nchembio.396

Supplementary Methods

Fluorophore absorbance and emission properties

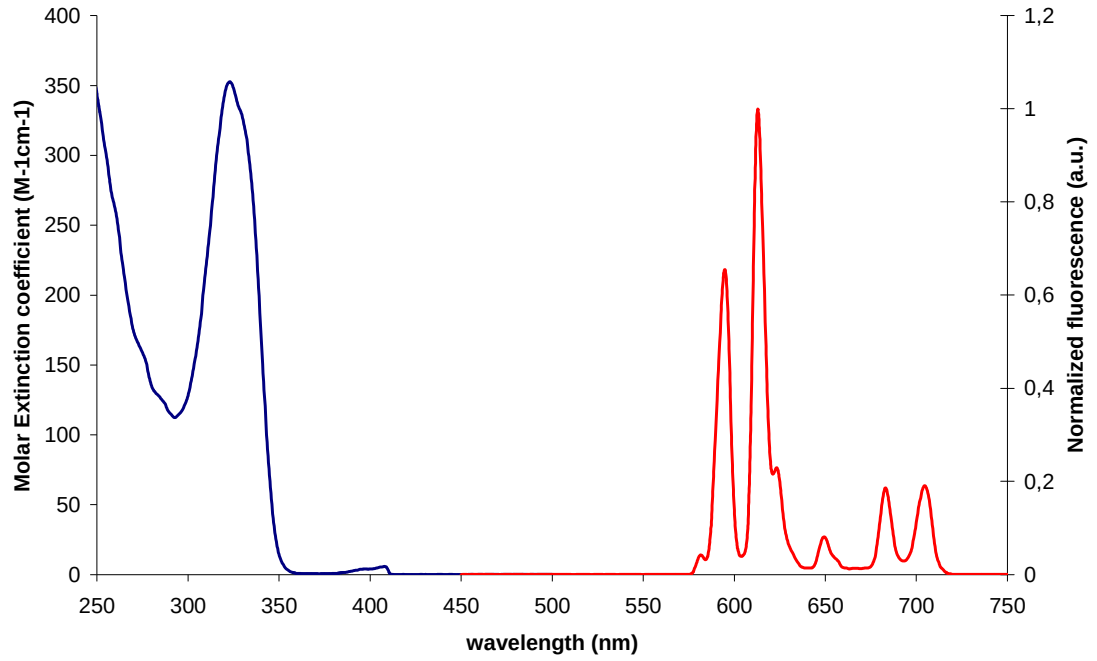

Supplementary Figure 4: Absorption and emission spectra of Eu-PBBP

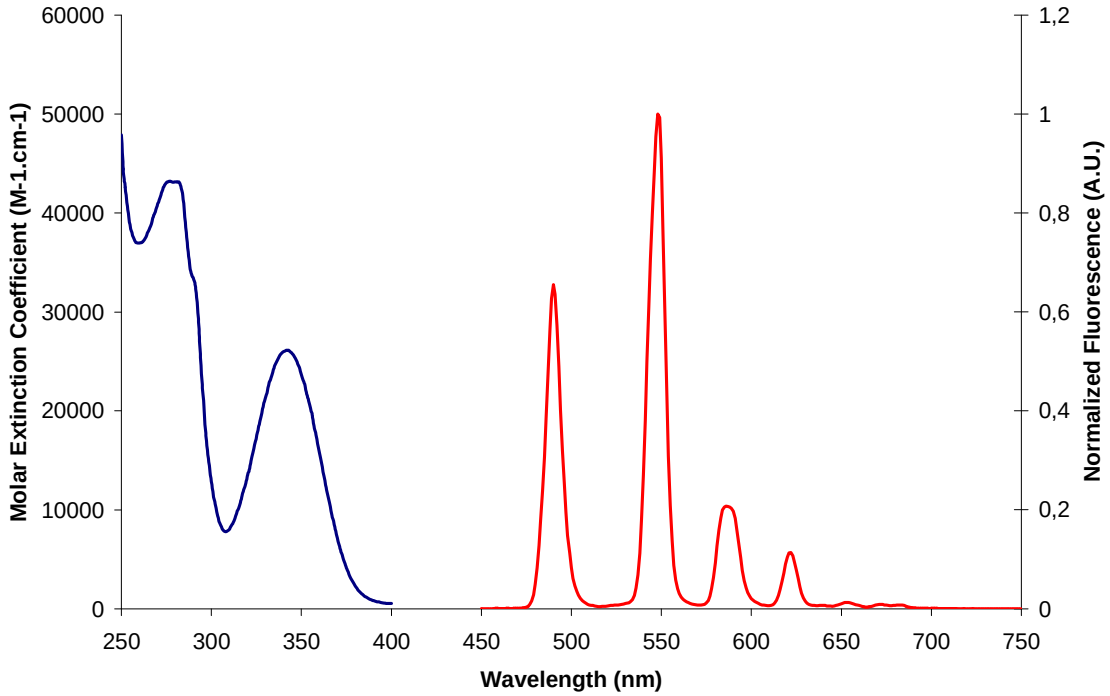

Supplementary Figure 5: Absorption and emission spectra of Lumi4-Tb

Nature Chemical Biology: doi: 10.1038/nchembio.396

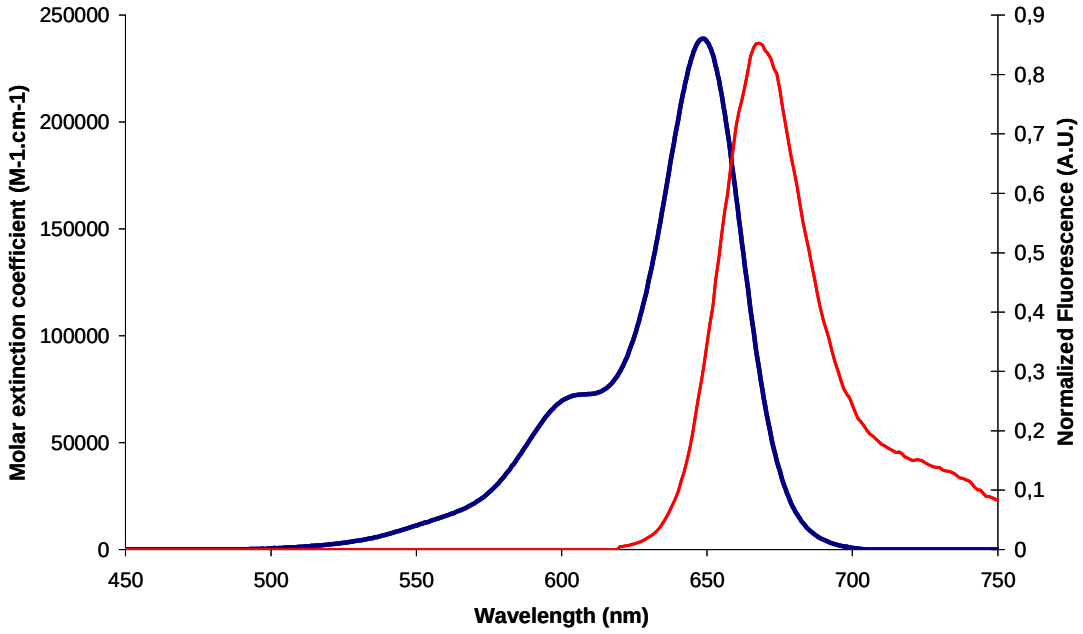

Supplementary Figure 6: Absorption and emission spectra of d1

Ligands syntheses

Peptide labeling with europium pyridine-bis-bipyridine cryptate fluorophores

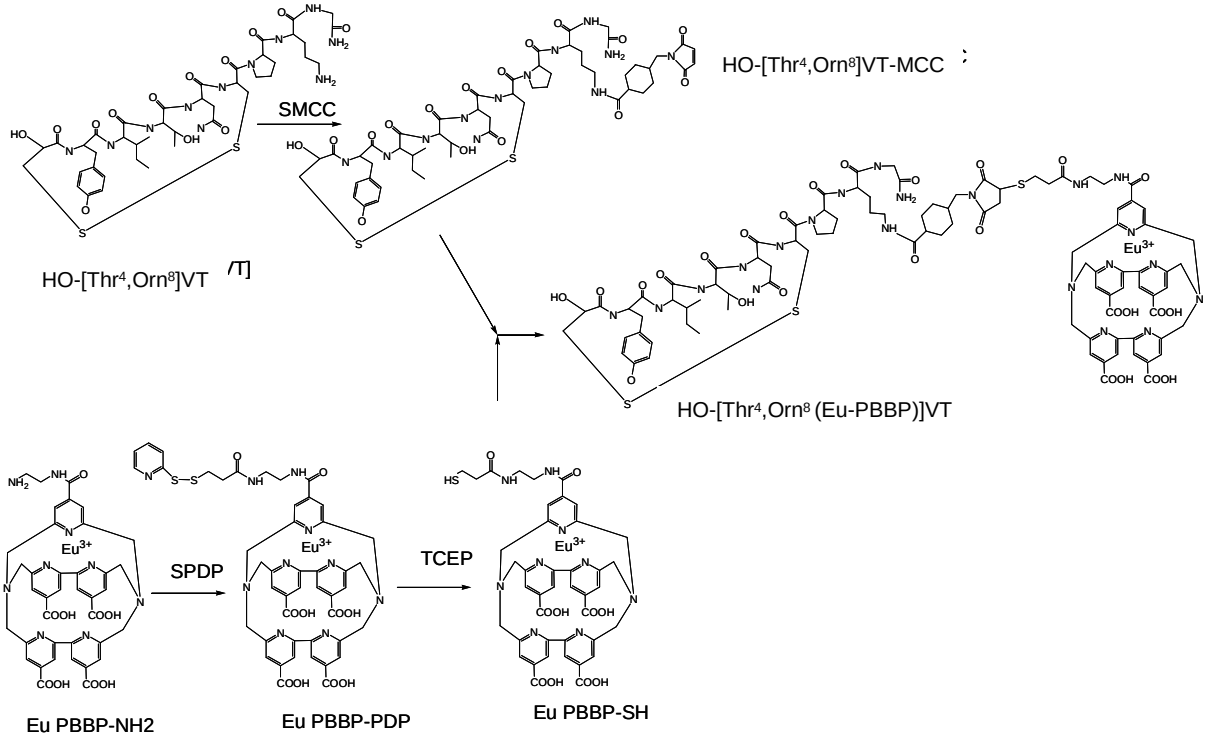

Nature Chemical Biology: doi: 10.1038/nchembio.396

Supplementary Figure 7: Protocol of fluorescent peptide synthesis illustrated here for the peptide HO-[Thr^4, Orn^8(Eu-PBBP)]VT cryptate conjugate

HPLC gradient A: 15% ACN in 0.2% aqueous TFA isocratic (5 min), linear gradient from 15%ACN to 55% ACN (15 min) 1mL/min. HPLC gradient B: 5% ACN in 0.2% aqueous TFA isocratic (5 min), linear gradient from 5%ACN to 55% ACN (15 min) 1mL/min. HPLC gradient C: 5% ACN in 0.1% aqueous formic acid isocratic (5 min), linear gradient from 5%ACN to 55% ACN (15 min) 1mL/min. HPLC gradient D: 10% ACN in 0.1% aqueous formic acid isocratic (1 min), linear gradient from 1% ACN to 65% ACN (14 min) 1mL/min.

The mass spectra were recorded on a Waters micromass-ZQ spectrometer, the UV-Visible spectra were recorded on a Beckman-Coulter DU800 spectrophotometer. HPLC were performed either on a Merck HPLC with L-6200 pump and L-4000 UV-Visible detector or a Waters Alliance 2695 HPLC system connected to a Waters 996 Diode Array Detector.

Synthesis of europium-pyridine-bis-bipyridine cryptate fluorophore

The Eu-PBBP-NH_2 cryptate was synthesized in-house[4]. RP-HPLC analysis: Lichrospher (Merck) 100 RP-18e (5 µm) 125 x 4 mm, 1mL / min, Merck L-4000 UV-vis detector set at 277 nm. Acceptor labeling : 1% aqueous TFA containing 5% ACN, 5 min isocratic, then linear gradient from 5% to 55% ACN in 15 min. Europium cryptate labeling : 1% aqueous TFA containing 15% ACN, 5 min isocratic, then linear gradient from 15% to 55% ACN in 15 min. Mass spectrometry was performed on a MALDI-TOF-TOF MS/MS (Ultreflex, Bruker) using ACCA as a matrix for MALDI ionization, or a Waters Micromass ZQ for electrospray (ES+) ionization. Eu-PBBP-NH_2 : MS (MALDI-TOF, matrix IDAA (trans-Indole Acrylic Acid (mass 187.19)) [M-H+IDAA] = 1098.8 (Calc. for $C_{38}H_{33}EuN_9O_9$; 912.16.)

Nature Chemical Biology: doi: 10.1038/nchembio.396

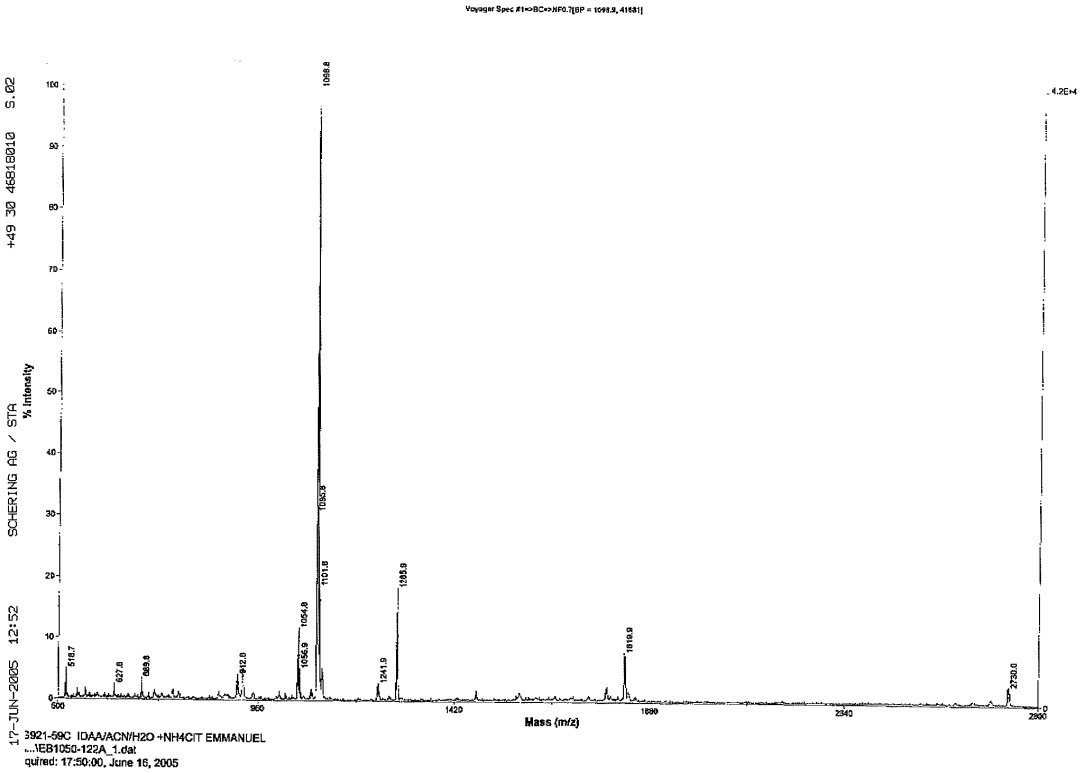

Supplementary Figure 8: Mass spectrum of Eu-PBBP-NH_2

Peptide labeling with europium pyridine-bis-bipyridine cryptate fluorophore

OH-[Thr^4, Orn^8 (Eu-PBBP)]VT cryptate conjugate (5)

The 2-hydroxy-3-mercaptopropanoic-Tyr-Ile-Thr-Asn-Cys-Pro-Orn-Gly-NH_2 cyclic 1-6 disulfide peptide HO-[Thr^4,Orn^8]VT, 5 mM in DMSO solution, was diluted with two volume of 100mM phosphate buffer pH7 and two molar equivalents of SMCC (10mM acetonitrile solution) were added. After 60 min at 20°C HPLC (Merck Lichrospher, RP18e , 4 x 125 mm gradient A) showed that the starting peptide (t_R = 13.2 min) was converted to the maleimide derivative tR = 16.2 min). The reaction was mixture was acidified (1% aqueous TFA) and the maleimide derivative was isolated using the same gradient, the resulting fraction was evaporated to dryness and stored at -20°C. UV (water) □max = 276 nm, 305 nm (ratio 305/267 = 0.34). The UV spectrum displays both a 277 nm absorption typical of the peptide scaffold and a 305 nm absorption characteristic of the maleimide residue. ESI (0.1% formic acid positive mode) $(M+ H)^+$ = 1201.6 Calc. 1200.5 for $C_{53}H_{76}N_{12}O_{16}S_2$. UV (0.1% aqueous formic acid): λmax 277 nm , 305 nm (A_{277}/A_{305} = 2.89).

Nature Chemical Biology: doi: 10.1038/nchembio.396

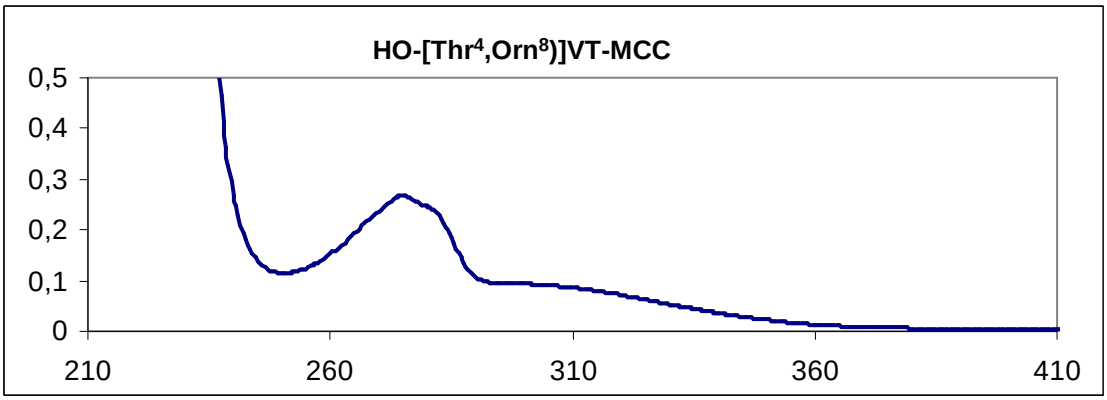

Supplementary Figure 9: absorbance spectrum of [OH^1] [Thr^4, Orn^8 VT]-MCC

The Eu⊂PBBP cryptate amine derivative (0.9 mg, 660 nmol) was dissolved in 250µL of HEPES buffer pH 7 and two equivalents of SPDP were added as a 5mM acetonitrile solution. The derivatization was monitored by RP-HPLC (Lichrospher gradient B). The starting cryptate (t_R = 2.4 min) was converted to the corresponding pyridyl-dithio-propanoyl derivative (t_R = 6.5 min) within 1 hour incubation at 20°C. The reaction mixture was acidified (1% aqueous TFA) and purified on chromolith column (gradient B) and the HPLC fractions were evaporated to dryness. ESI (0.1% formic acid positive mode): $(M\text{-}H+HCOOH)^{2+}$ / 2 = 577.29 & 577.26 , $(M+HCOOH)^{3+}$ / 3 = 385.15 , $(M\text{-}H+CF_3COOH)^{2+}$ / 2 = 610.28 & 611.19. Calc. 1109.16 (100.0%), 1107.16 (79.2%) for $EuC_{46}H_{40}N_{10}O_{10}S_2$. The doubly charged species show peaks as m/z = 576.29 & 577.26 arising from the isotopic europium profile (two isotopes ^{151}Eu and ^{153}Eu of roughly equal abundance).

The pyridyl-dithio-propanoyl Eu-PBBP cryptate **17** was dissolved in HEPES buffer pH 7 (250 nmol in 100 µL) and five equivalent of TCEP (0.1M aqueous solution) were added. The starting compound (t_R = 6.5 min) was converted to the Eu-PBBP cryptate thiol derivative (t_R = 5.2 min) within one hour incubation at 20°C. The reaction mixture was acidified, purified on chromolith column (gradient B) and the HPLC fractions were evaporated to dryness. The resulting Eu-PBBP cryptate thiol derivative was aliquoted (screw cap eppendorf tubes) by evaporation to dryness (speed-vac) and stored at -20°C.

ESI (0.1% formic acid positive mode): $(M\text{-}H+HCOOH)^{2+}$ / 2 = 521.84 & 522.68 Calc. 1000.16 (100.0%) 998.16, (81.5%) for $C_{41}H_{37}EuN_9O_{10}S$. The doubly charged species show two peaks arising from the europium isotopic profile.

To the above maleimide derivatized peptide, 240 µM in 50mM phosphate buffer (pH6), was added 1.2 equivalent of Eu-PBBP cryptate thiol derivative. After 16h incubation (20°C) the

Nature Chemical Biology: doi: 10.1038/nchembio.396

medium was acidified (0.1% TFA) and purified on RP-HPLC (Lichrospher gradient A). The Eu-PBBP labeled peptide was isolated (t_R = 14.9 min) and the fraction evaporated to dryness. UV (water): □max 326 nm. ESI (0.1% formic acid positive mode) m/z: $(M- H)^{2+}$ / 2 = 1100.0, $(M)^{3+}$ / 3 = 733.8 . Calc. 2201.2 for $C_{94}H_{113}EuN_{21}O_{26}S_3$. Upon storage (phosphate buffer pH7) we observed an opening of the thiosuccinimide ring upon addition of one molecule of water yielding a compound eluting 0.5 min earlier on RP-HPLC. Such ring opening is known to occur in the conjugates prepared through thiol-maleimide coupling.

ESI (0.1% formic acid positive mode) m/z : $(M- H)^{2+}$ / 2 = 1109.0 , $(M)^{3+}$ / 3 = 739.6 . Calc. 2219.2 for $C_{94}H_{115}EuN_{21}O_{27}S_3$.

Characterization of the compounds

HO-[Thr^4, Orn^8]VT-Maleimide

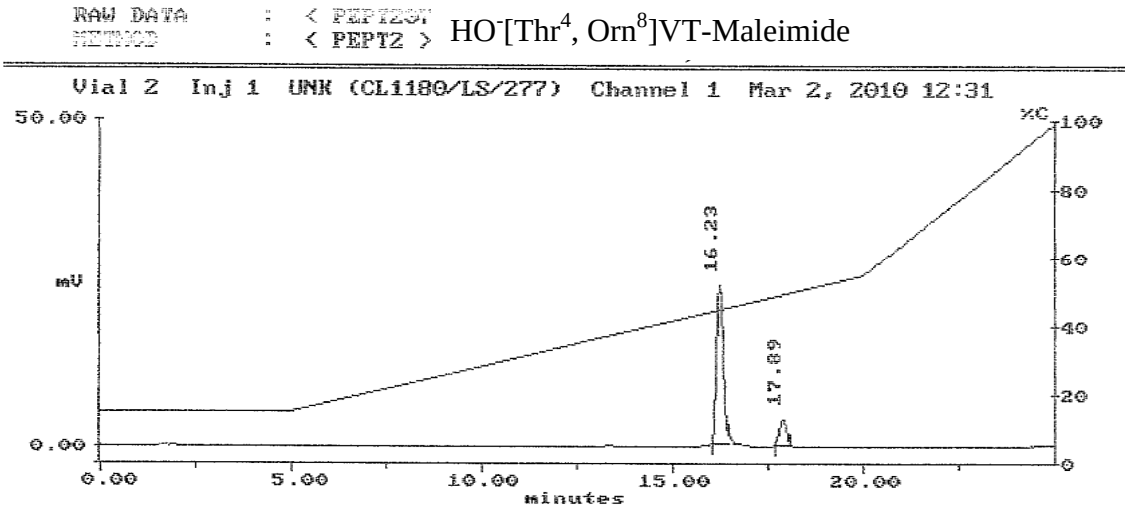

Supplementary Figure 10: HPLC spectrum of HO-[Thr^4, Orn^8]VT-Maleimide

Nature Chemical Biology: doi: 10.1038/nchembio.396

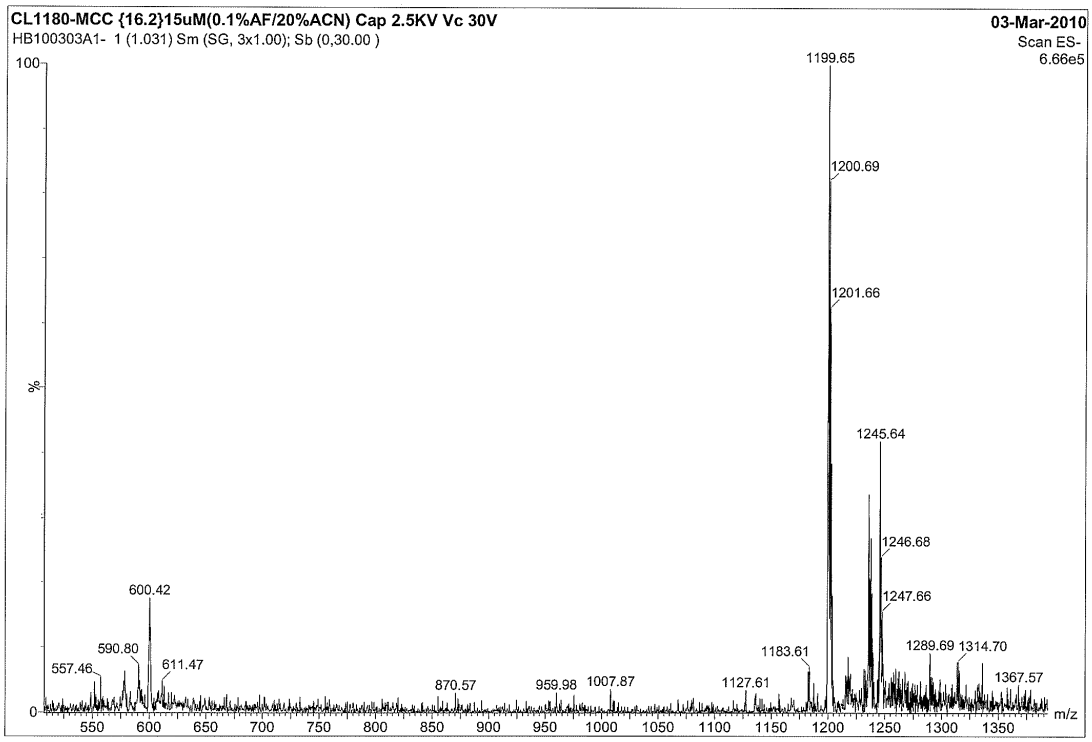

Supplementary Figure 11: Mass spectrum of HO-[Thr^4, Orn^8]VT-Maleimide

Eu-PBBP-NH_2

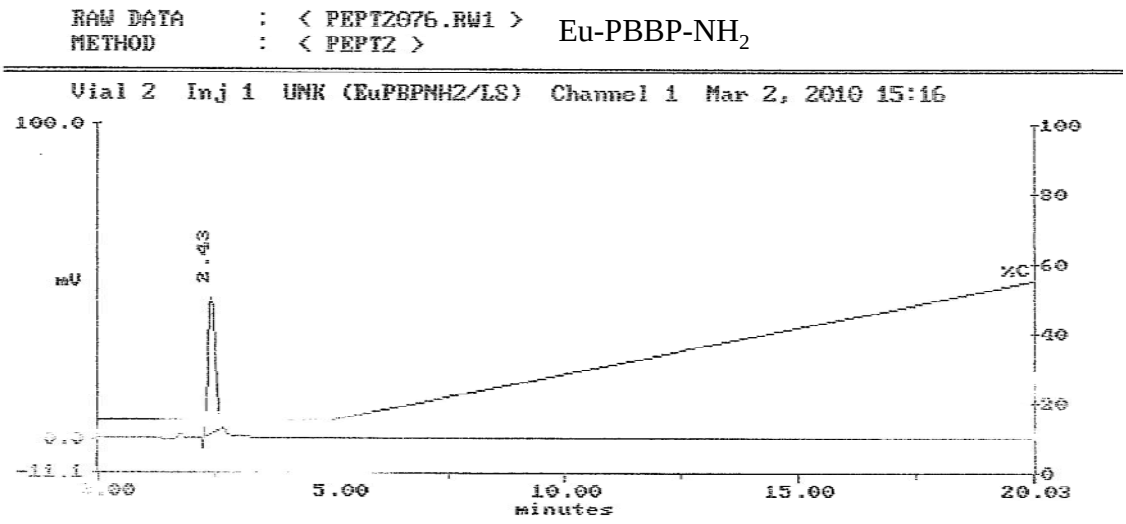

Supplementary Figure 12: HPLC spectrum of Eu-PBBP-NH_2

Nature Chemical Biology: doi: 10.1038/nchembio.396

Eu-PBBP-pyridyldithiopropanoyl

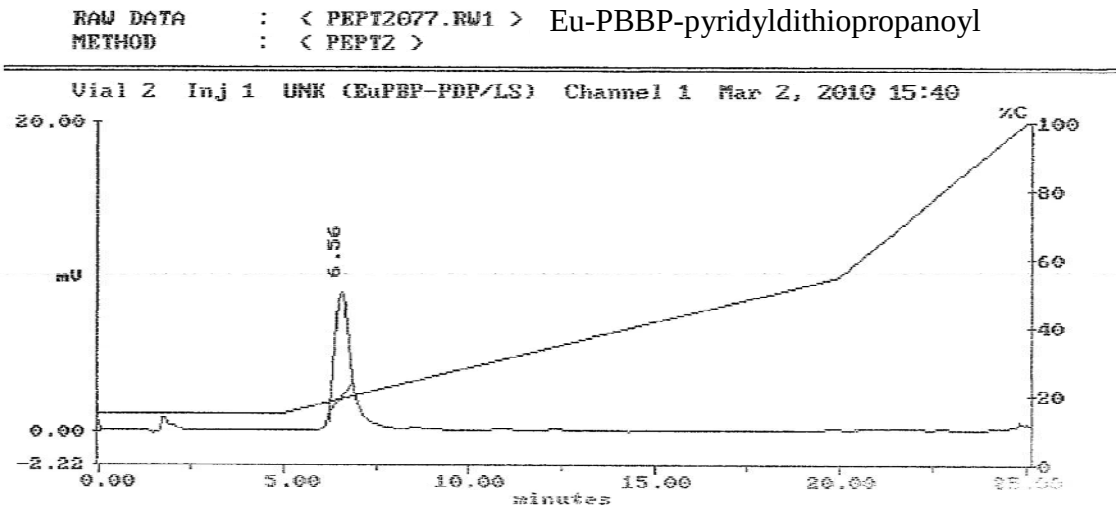

Supplementary Figure 13: HPLC spectrum of Eu-PBBP-pyridyldithiopropanoyl

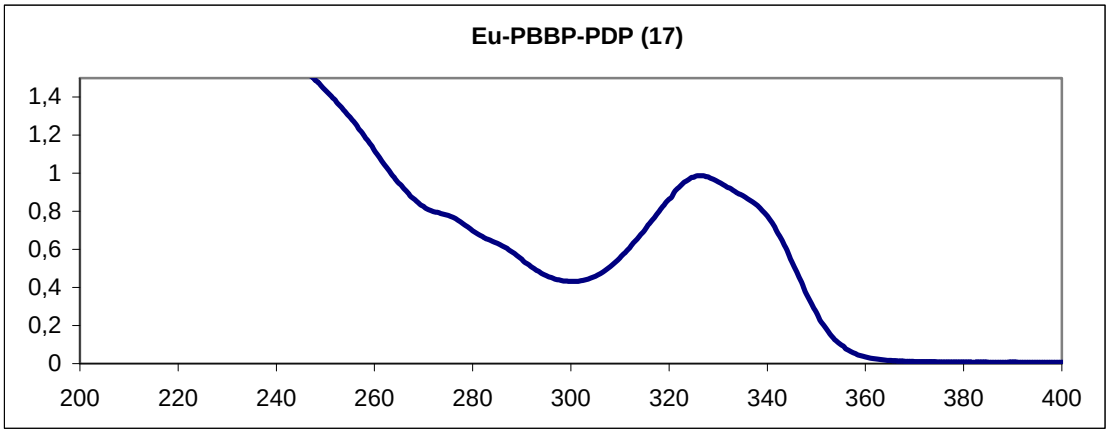

Supplementary Figure 14: absorbance spectrum of Eu-PBBP-pyridyldithiopropanoyl. Absorbance peak at 327 nm

Nature Chemical Biology: doi: 10.1038/nchembio.396

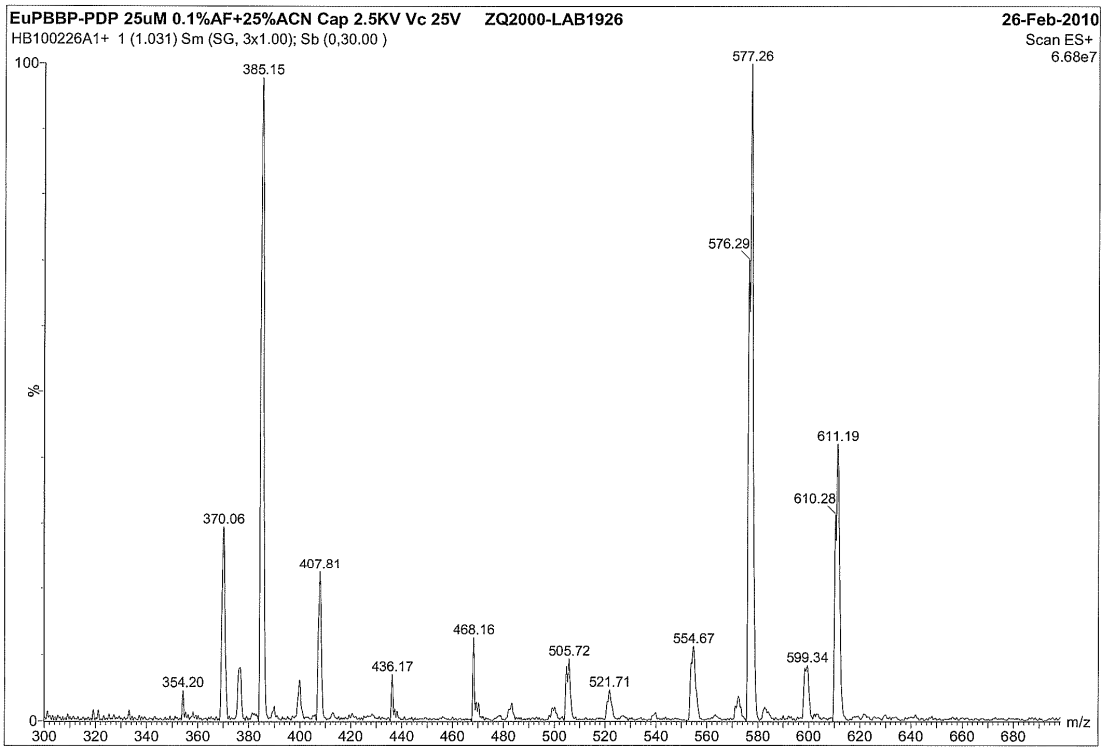

Supplementary Figure 15: Mass spectrum of Eu-PBBP-pyridyldithiopropanoyl

Eu-PBBP-SH

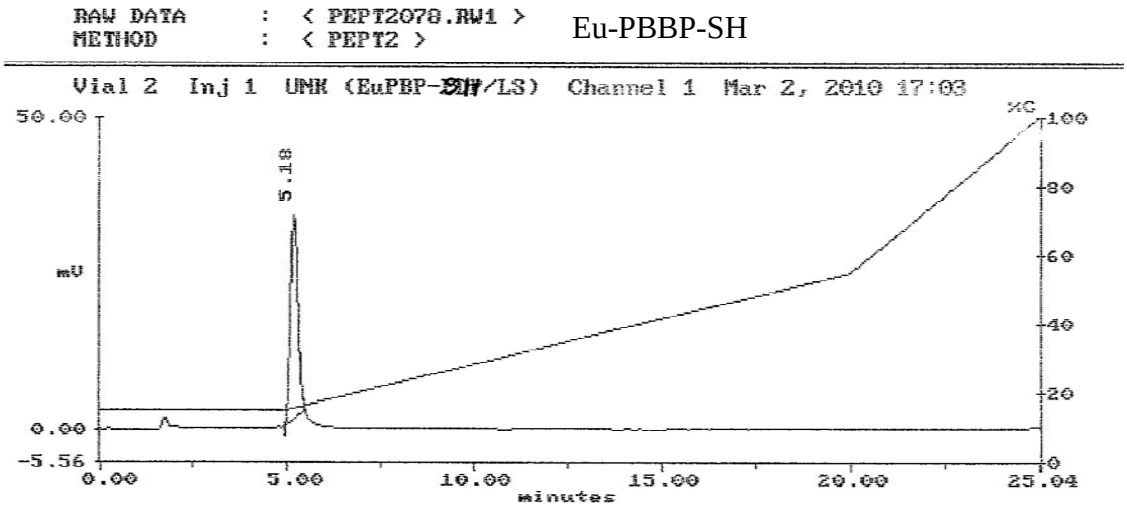

Supplementary Figure 16: HPLC spectrum of Eu-PBBP-SH

Nature Chemical Biology: doi: 10.1038/nchembio.396

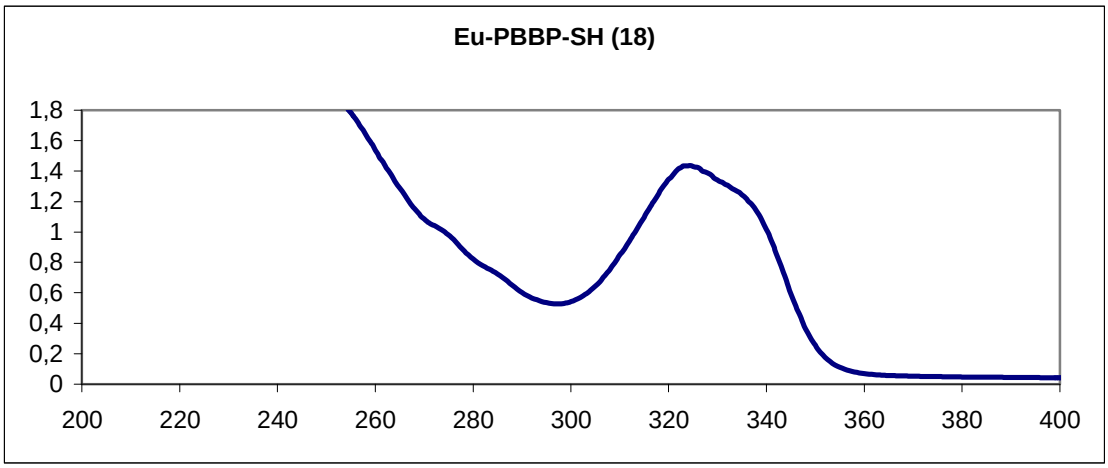

Supplementary Figure 17: absorbance spectrum of Eu-PBBP-SH. Absorbance peak at 325 nm

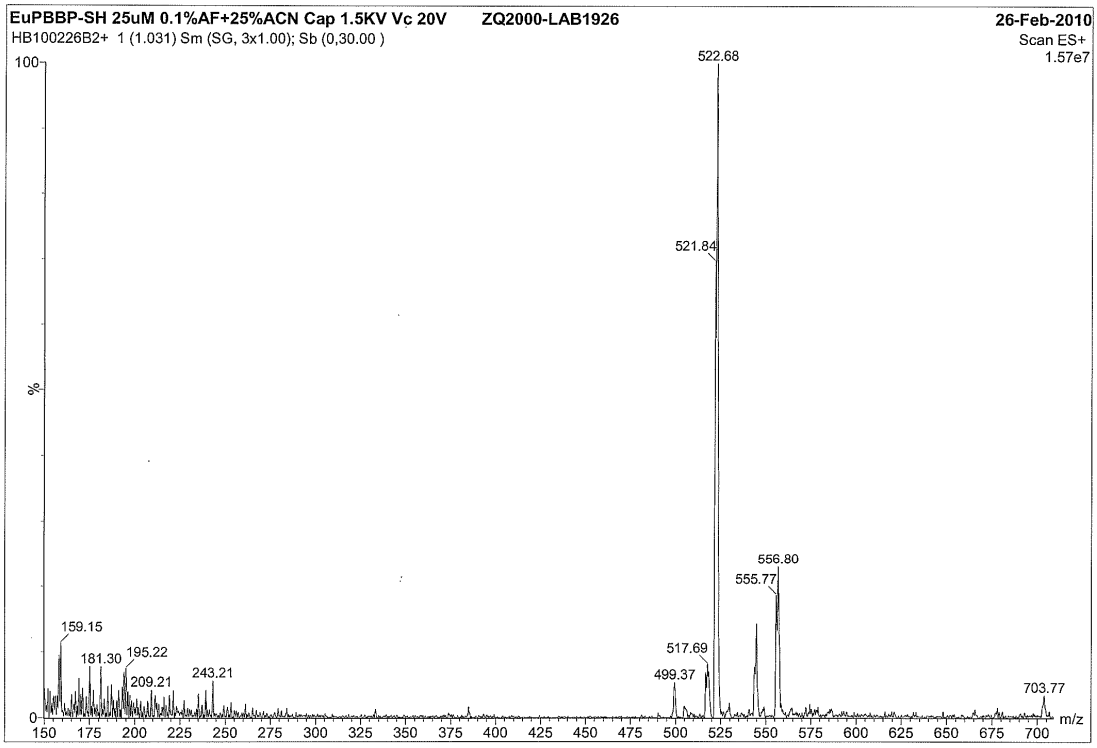

Supplementary Figure 18: Mass spectrum of Eu-PBBP-SH

Nature Chemical Biology: doi: 10.1038/nchembio.396

[HO[1]][Thr[4],Orn[8](Eu-PBBP)]VT (**5**)

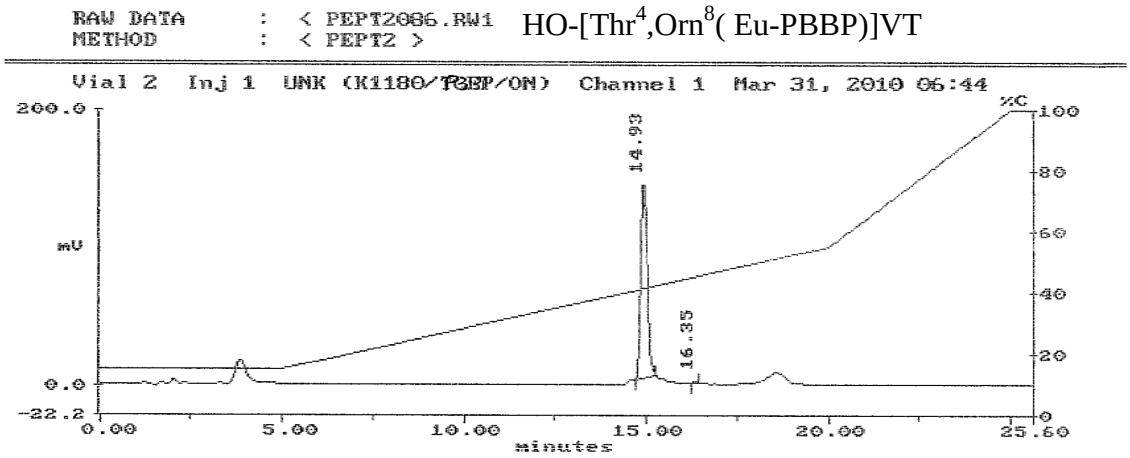

Supplementary Figure 19: HPLC spectrum of HO-[Thr[4],Orn[8](Eu-PBBP)]VT (**5**)

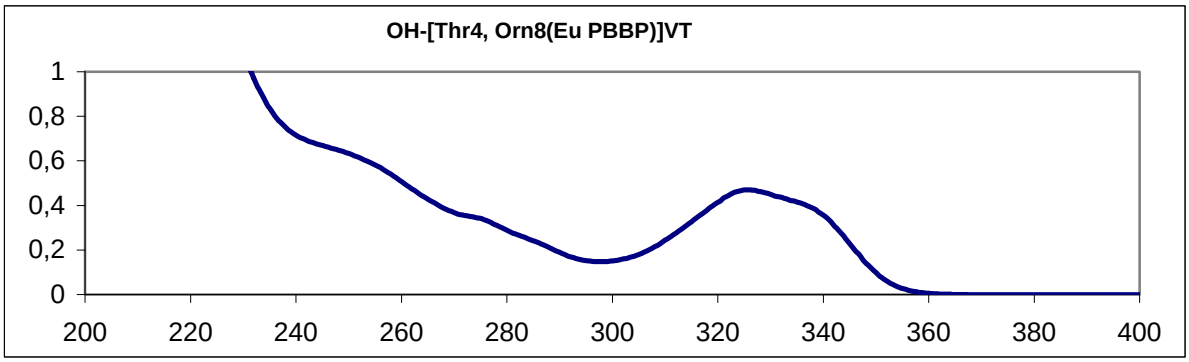

Supplementary Figure 20: absorbance spectrum of HO-[Thr[4],Orn[8](Eu-PBBP)]VT (**5**). Absorbance peak at 326 nm

Nature Chemical Biology: doi: 10.1038/nchembio.396

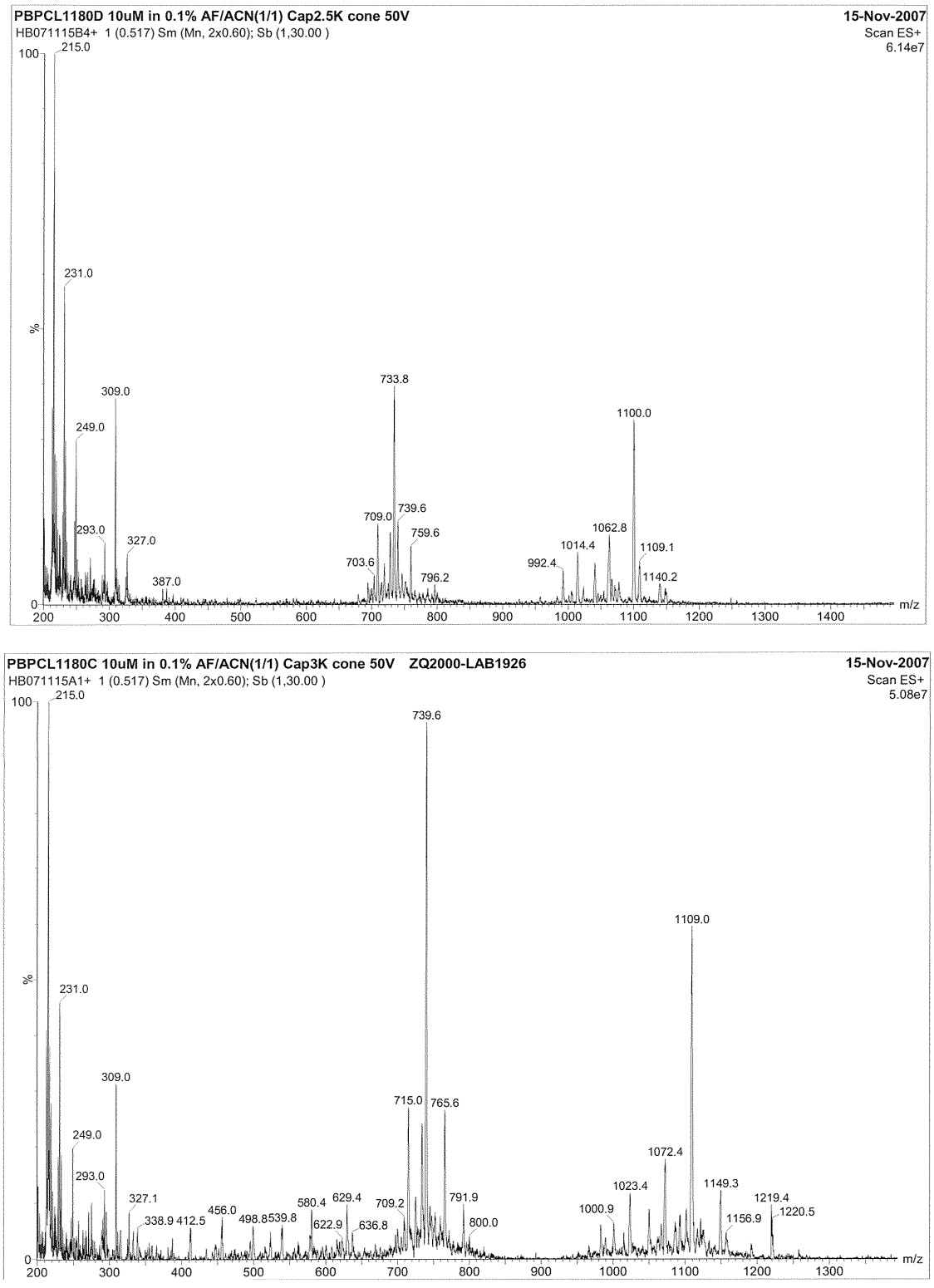

Supplementary Figure 21: Mass spectra of HO-[Thr^4,Orn^8 (Eu-PBBP)]VT (**5**).

Nature Chemical Biology: doi: 10.1038/nchembio.396

4-HOPh$(CH_2)_2$CO-D-Tyr(Me)-Phe-Gln-Asn-Arg-Pro-Lys(Eu-PBBP)-NH_2, cryptate conjugate ([Lys^8(Eu-PBBP)]PVA cryptate conjugate) (1):

The [Lys8] PVA peptide [phenylpropionic linear vasopressin antagonist, 4-HOPh$(CH_2)_2$CO-DTyr(Me)-Phe-Gln-Asn-Arg-Pro-Lys-NH_2 [5] was labelled and purified as described above. RP-HPLC (Lichrospher RP18e, gradient A) t_R =17.5min. MS consistent with previously reported data [Albizu J. Med. Chem. 2007, 50(20): 4976-85]

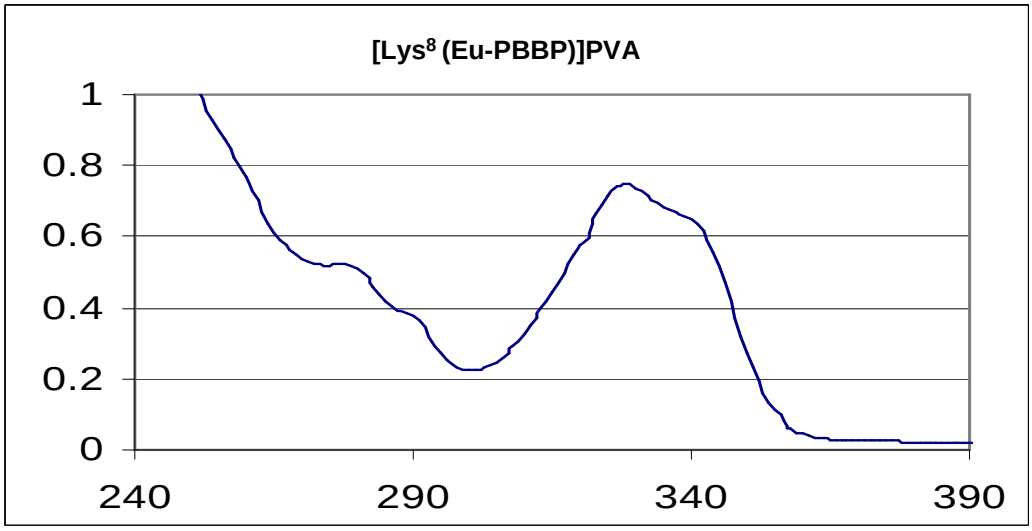

Supplementary Figure 22: absorbance spectrum of [Lys^8(Eu-PBBP)]PVA (**1**). Absorbance peak at 327 nm.

Peptide labeling with Alexa fluorophore

HO-[Thr^4, Orn^8(Alexa 647)]VT (6)

To the 2-hydroxy-3-mercaptopropanoic-Tyr-Ile-Thr-Asn-Cys-Pro-Orn-Gly-NH_2 cyclic 1-6 disulfide peptide [OH^1] [Thr^4, Orn^8 VT] previously described[6], 5 mM in DMSO solution was added 1.5 equivalent of Alexa 647 succinimidyl ester (Invitrogen, France) (10 mM DMSO solution) and 3 equivalent of i-Pr_2EtN (0.1 M DMSO solution) and mixed (Vortex). After 1 h, analytical RP-HPLC on Xbridge column (Waters Xbridge C18 3.5µ 4.6x100 mm, gradient C detection at 280 nm) showed residual peptide peak at t_R =15.5 min, a new slightly more hydrophilic compound t_R =14.4 min and hydrolysed Alexa 647 species (t_R =12.5 and 12.8 min). The Alexa 647 labelled [OH^1] [Thr^4, Orn^8 VT] peptide was isolated by RP-HPLC on Xbridge (gradient C). ESI (0.1% formic acid negative mode): $(M-2H)^{2-}/2$ = 910.47 , $(M-3H)^{3-}/3$ = 606.79 (Alexa 647 structure not available).

Nature Chemical Biology: doi: 10.1038/nchembio.396

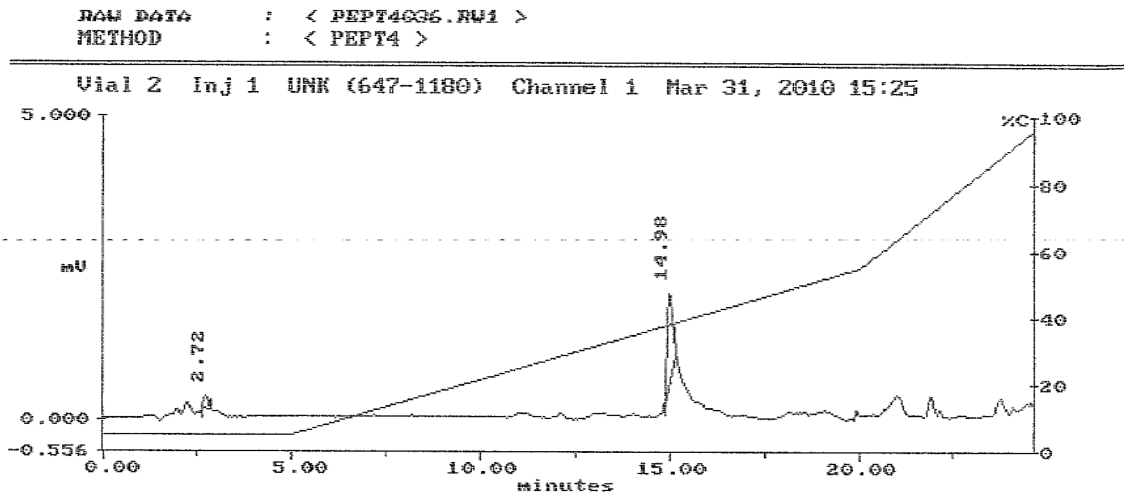

Supplementary Figure 23: HPLC spectrum of HO-[Thr^4, Orn^8(Alexa 647)]VT (**6**)

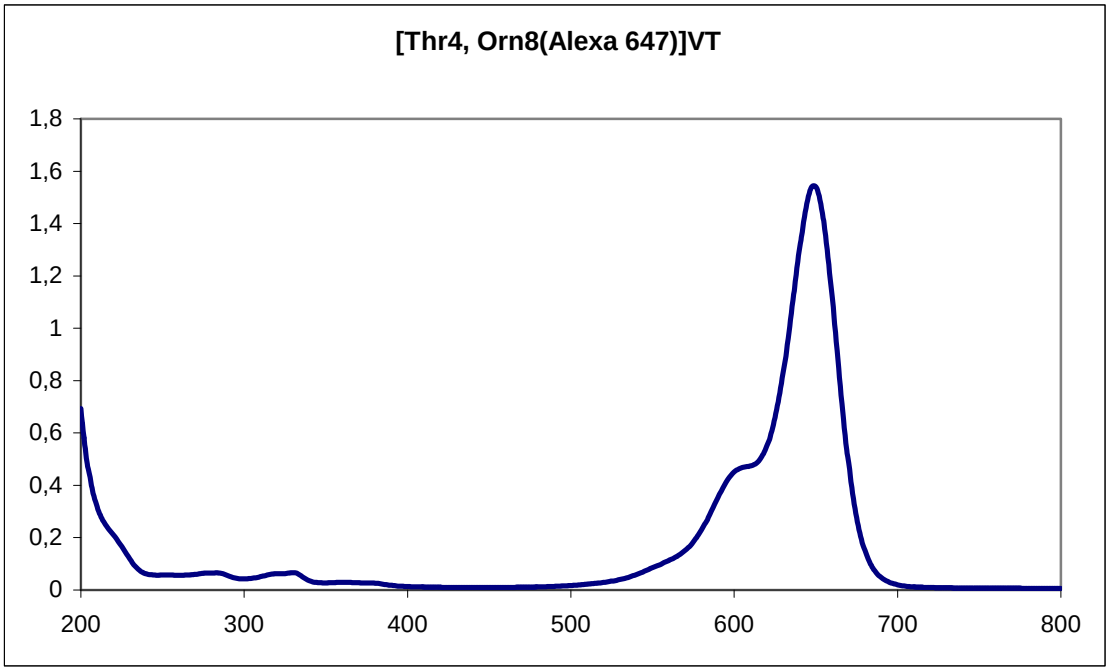

Supplementary Figure 24: absorbance spectrum of HO-[Thr^4, Orn^8(Alexa 647)]VT (**6**). Absorbance peak at 647 nm

Nature Chemical Biology: doi: 10.1038/nchembio.396

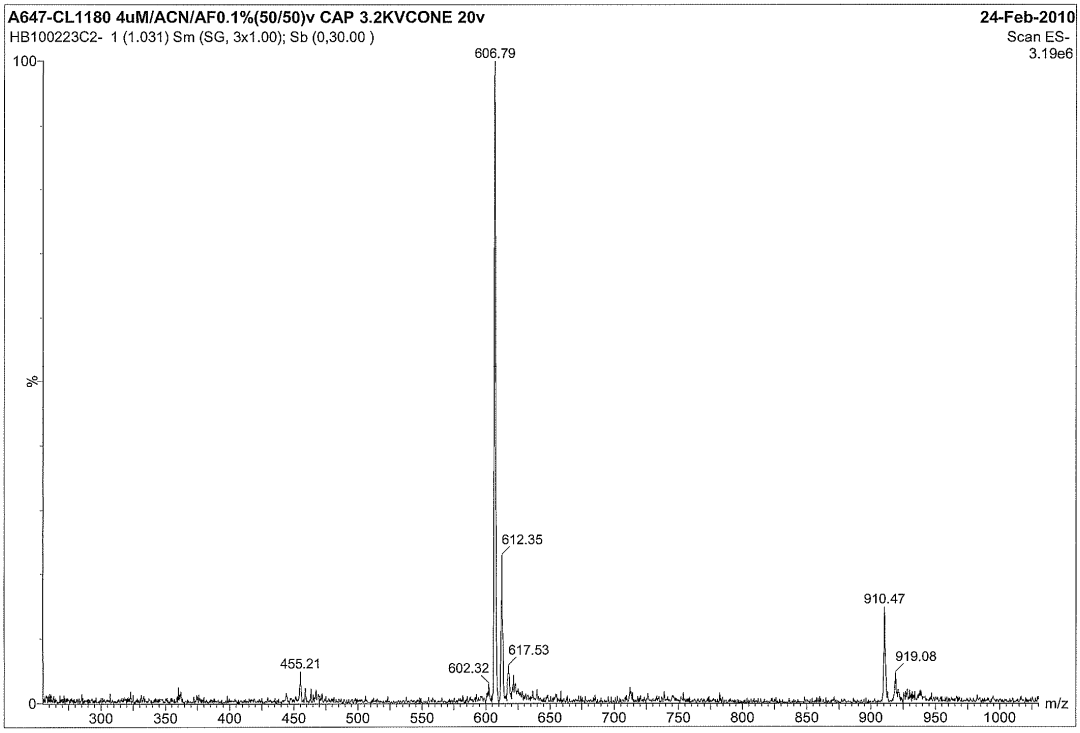

Supplementary Figure 25: mass spectrum of HO-[Thr^4, Orn^8(Alexa 647)]VT (**6**)

4-HOPh$(CH_2)_2$CO-DTyr(Me)-Phe-Gln-Asn-Arg-Pro-Lys (Alexa 647)-NH_2 ([Lys8(Alexa 647)]PVA) (**2**)

The [Lys8] PVA peptide [phenylpropionic linear vasopressin antagonist, 4-HOPh$(CH_2)_2$CO-DTyr(Me)-Phe-Gln-Asn-Arg-Pro-Lys-NH_2] was labelled with Alexa 647 NHS as described above. RP-HPLC (Waters Xbridge C18 3.5µ 4.6x100 mm, gradient D) t_R =8.18 min. ESI (0.1% formic acid positive mode) m/z: $(M+2H)^{2+}$ / 2 = 977.85 (Alexa 647 structure not available).

Nature Chemical Biology: doi: 10.1038/nchembio.396

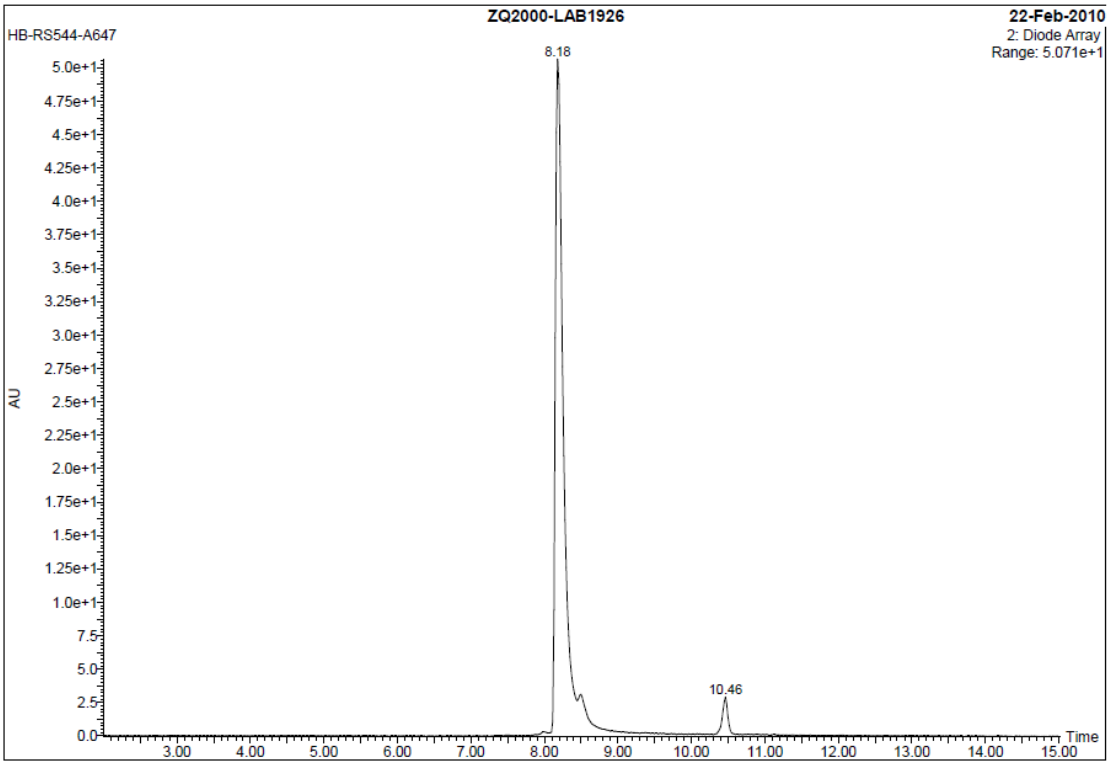

Supplementary Figure 26: HPLC spectrum of [Lys^{8}(Alexa 647)]PVA (**2**)

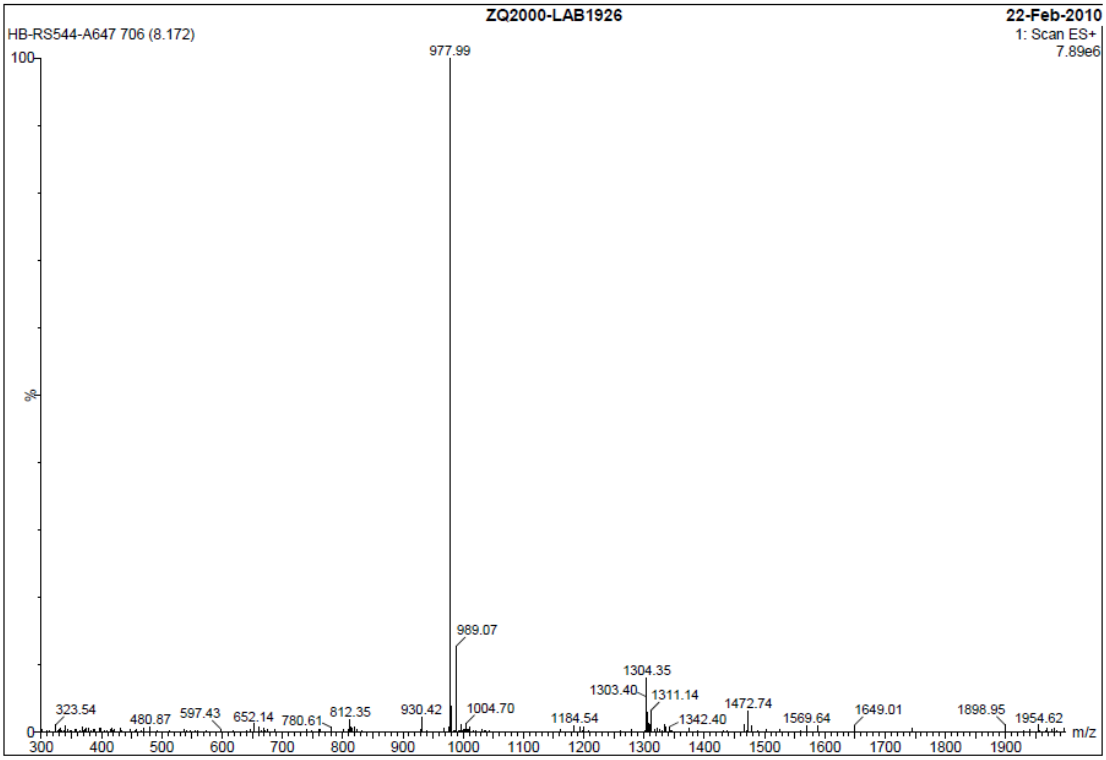

Supplementary Figure 27: mass spectrum of [Lys^{8}(Alexa 647)]PVA (**2**)

Nature Chemical Biology: doi: 10.1038/nchembio.396

Peptide labeling with Lumi4-Tb™ fluorophore

Lumi4-Tb™ -NHS was synthesized by CisBio Bioassays.

4-HOPh$(CH_2)_2$CO-DTyr(Me)-Phe-Gln-Asn-Arg-Pro-Lys(Lumi4-Tb)-NH_2 ([Lys8(Lumi4-Tb)]PVA) (**13**)

To 4-HOPh$(CH_2)_2$CO-DTyr(Me)-Phe-Gln-Asn-Arg-Pro-Lys)-NH_2 (0.7 mg - 650 nmol – 1 eq) in dry DMSO (200 µL) was added Lumi4-Tb™ -NHS (650 nmol – 1 eq) in dry DMSO (30 µL) and diisopropylethylamine (0.35 µL – 2 µmol- 3 eq). The mixture was stirred at room temperature for 1 h. After this period the reaction was completed. Purification was performed by preparative HPLC using water 25 mM triethylammonium acetate pH 7 as eluent with acetonitrile gradient to give 250 nmol of the desired product (38 % yield).. Mass spectra was recorded by ES ionization on a Waters Micromass *m/z* ($HRMS^+$) 1264.6504 $[M]^+/2$ ($C_{118}H_{158}N_{27}O_{26}Tb$) Calcd 1264.0557.

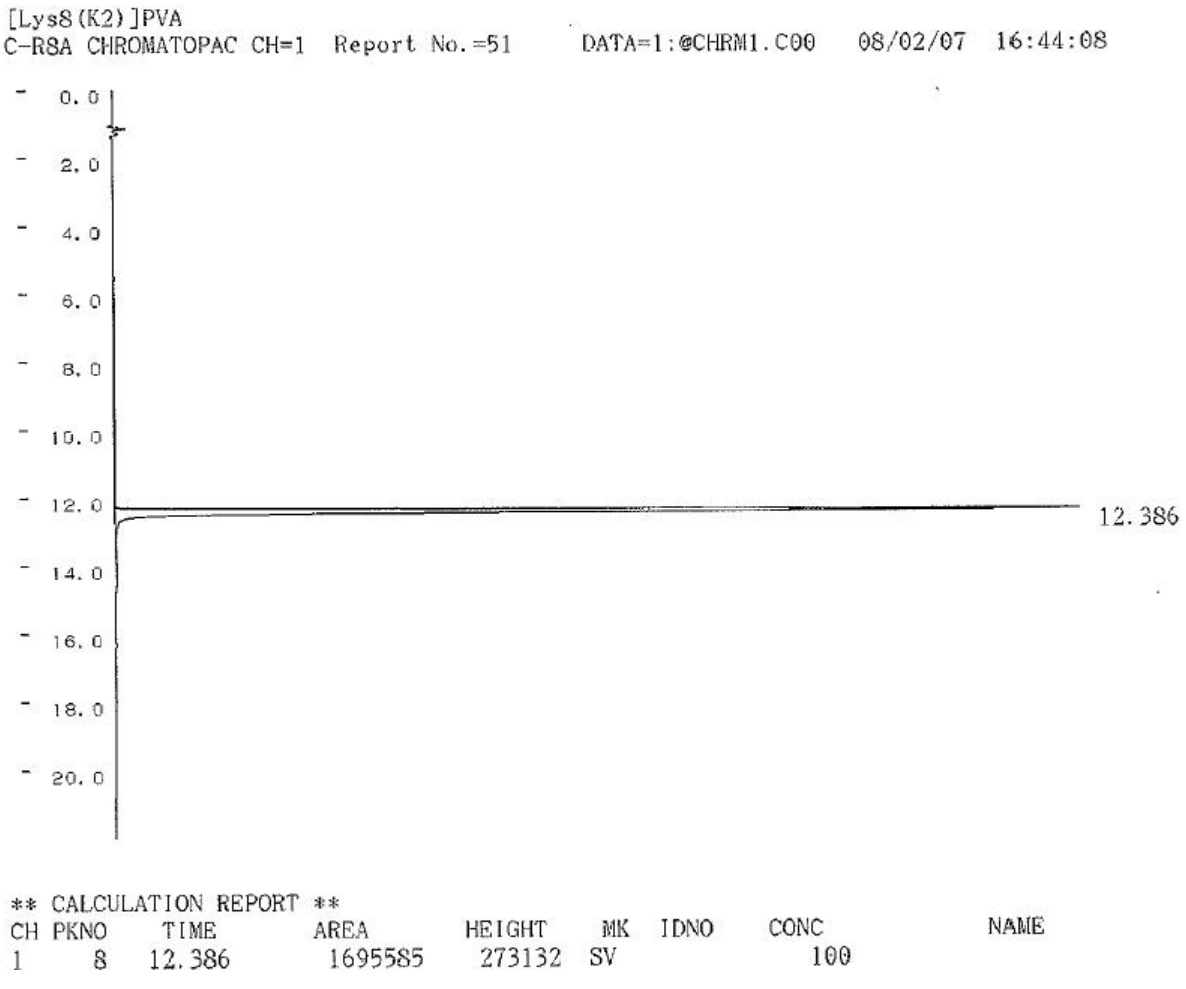

Supplementary Figure 28: HPLC spectrum of [Lys^8(Lumi4-Tb)]PVA (**13**)

Nature Chemical Biology: doi: 10.1038/nchembio.396

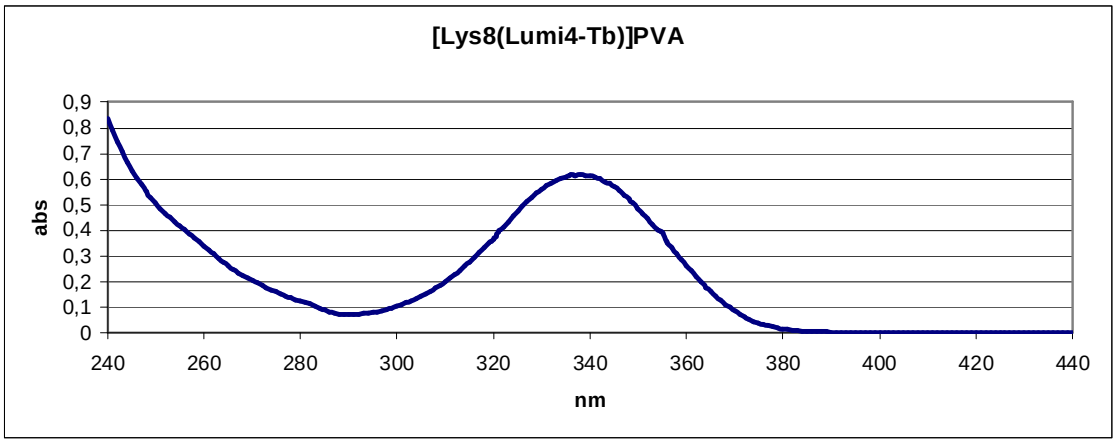

Supplementary Figure 29: absorbance spectrum of [Lys[8](Lumi4-Tb)]PVA (**13**). Absorbance peak at 338 nm.

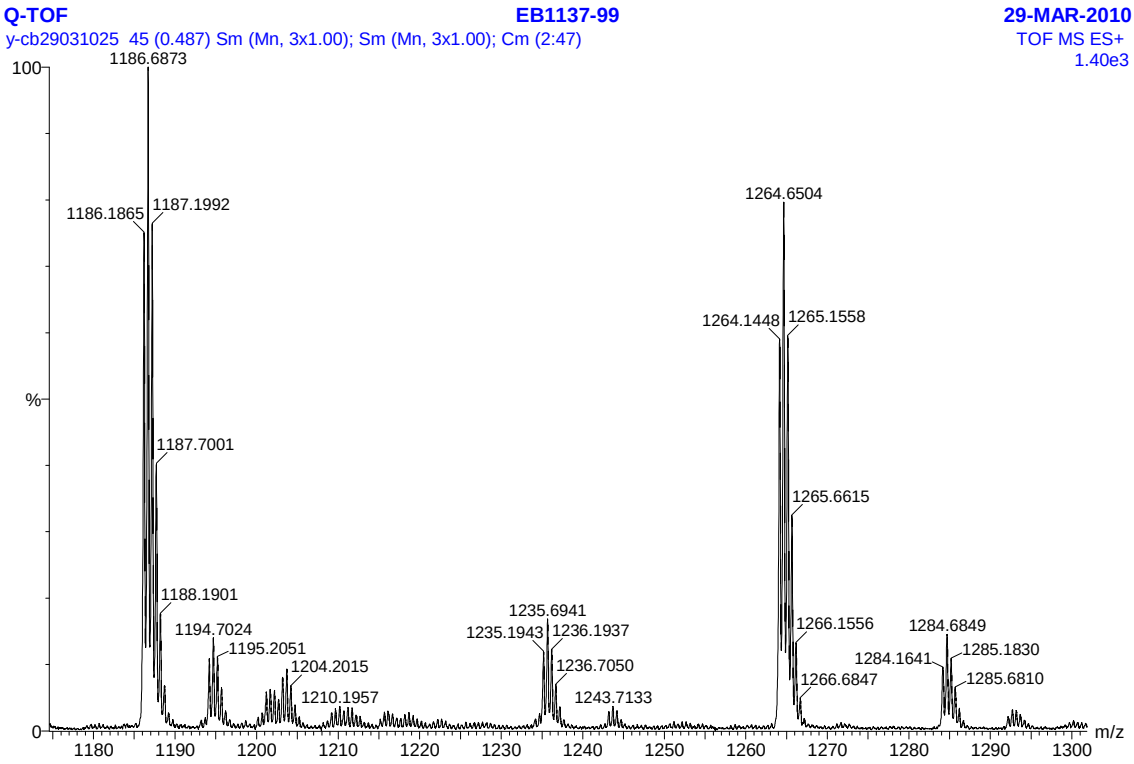

Supplementary Figure 30: Mass spectrum of [Lys[8](Lumi4-Tb)]PVA (**13**).

V_2 antagonist peptide d$(CH_2)_5$-DTyr(Et)-Phe-Ile-Asn-Cys-Pro-Arg-Eda labeling

Nature Chemical Biology: doi: 10.1038/nchembio.396

Peptide d$(CH_2)_5$-DTyr(Et)-Phe-Ile-Asn-Cys-Pro-Arg-Eda was synthesized as previously described [7].Alexa 488-NHS was purchased from Invitrogen.

Peptide labeling with Lumi4-Tb™ fluorophore: d$(CH_2)_5$[DTyr(Et)^2, Ile^4, Eda(Lumi4-Tb)^9]VP (3)

To the peptide (1.1 mg - 1 µmol) in 50 mM phosphate buffer pH 8 (2 mL) was added Lumi4-Tb™ -NHS (1 µmol) in dry DMSO (100 µL). The mixture was stirred at room temperature for 1 h. After this period the reaction was completed. Purification was performed by preparative HPLC using water 25 mM triethylammonium acetate pH 7 as eluent with acetonitrile gradient to give 100 nmol of the desired product (25 % yield). MS : m/z2+ = 1276.28.

Acquired: 10/09/2009 13:42:28
Printed: 10/09/2009 15:37:38

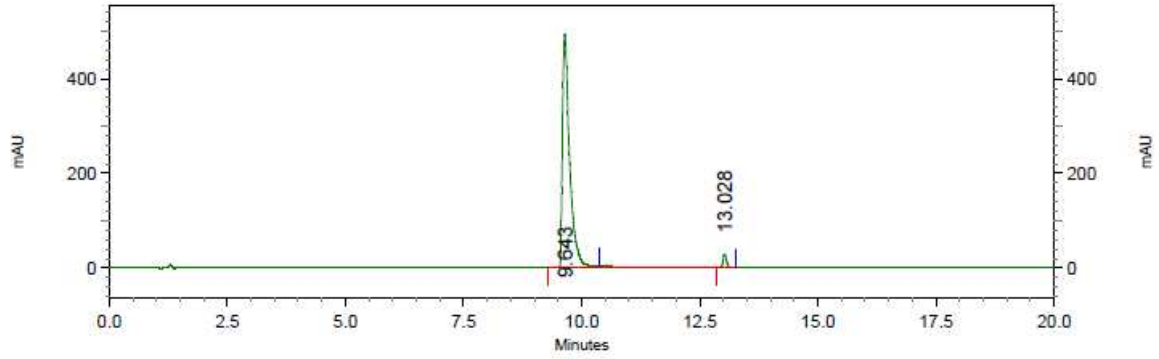

UV2000-320nm
Results (eb
(10/09/2009
15:36:54)
(Reprocessed))

Retention Time	Area	Area %	Height	Height %
9.643	5226360	97.17	494456	94.41
13.028	152424	2.83	29256	5.59
Totals	5378784	100.00	523712	100.00

Supplementary Figure 31: HPLC spectrum of d$(CH_2)_5$[DTyr(Et)^2, Ile^4, Eda(Lumi4-Tb)^9]VP (**3**)

Nature Chemical Biology: doi: 10.1038/nchembio.396

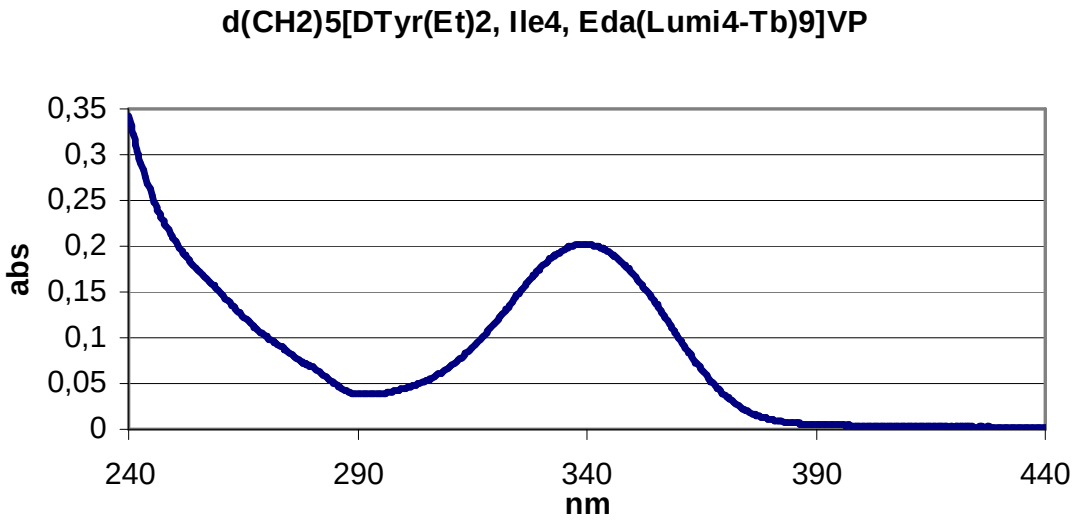

Supplementary Figure 32: Absorbance spectrum of d$(CH_2)_5$[DTyr(Et)^2, Ile^4, Eda(Lumi4-Tb)^9]VP (**3**). Absorbance peak at 339 nm.

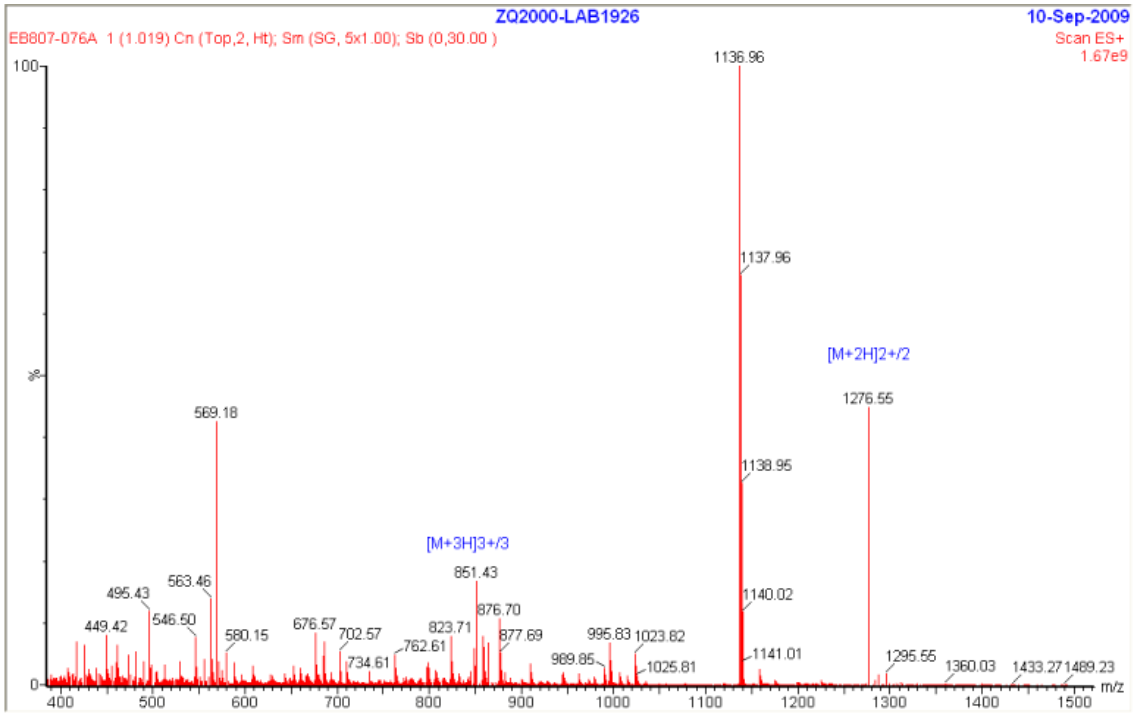

Supplementary Figure 33: Mass spectrometry characterization of d$(CH_2)_5$[DTyr(Et)^2, Ile^4, Eda(Lumi4-Tb)^9]VP (**3**).

Peptide labeling with Alexa 488 fluorophore: d$(CH_2)_5$[DTyr(Et)^2, Ile^4, Eda(Alexa 488)^9]VP (4)

Nature Chemical Biology: doi: 10.1038/nchembio.396

To the peptide (1.1 mg - 1 µmol) in 50 mM phosphate buffer pH 8 (2 mL) was added Alexa 488-NHS (1 µmol) in dry DMSO (100 µL). The mixture was stirred at room temperature for 1 h. After this period the reaction was completed. Purification was performed by preparative HPLC using water 0.2 % trifluoroacetic acid as eluent with acetonitrile gradient to give 250 nmol of the desired product (25 % yield). Mass spectra was recorded by ES ionization on a Waters Micromass ZQ 2000 *m/z* = 1653.42**.**

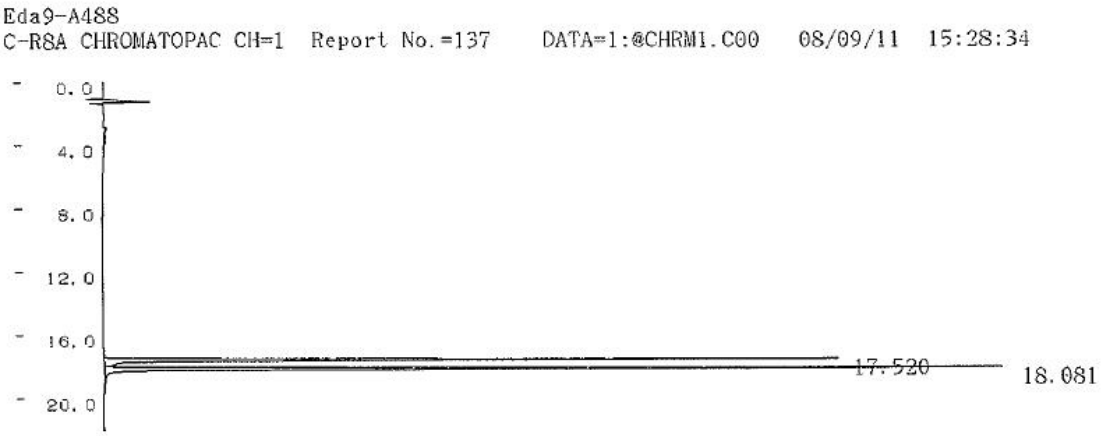

** CALCULATION REPORT **

CH	PKNO	TIME	AREA	HEIGHT	MK	IDNO	CONC	NAME
1	3	17.52	683822	105092	SV		44.2284	
	5	18.081	862293	138382	V		55.7716	
		TOTAL	1546114	243475			100	

Supplementary Figure 34: HPLC spectrum of d$(CH_2)_5$[DTyr(Et)^2, Ile^4, Eda(Alexa 488)^9]VP (**4**)

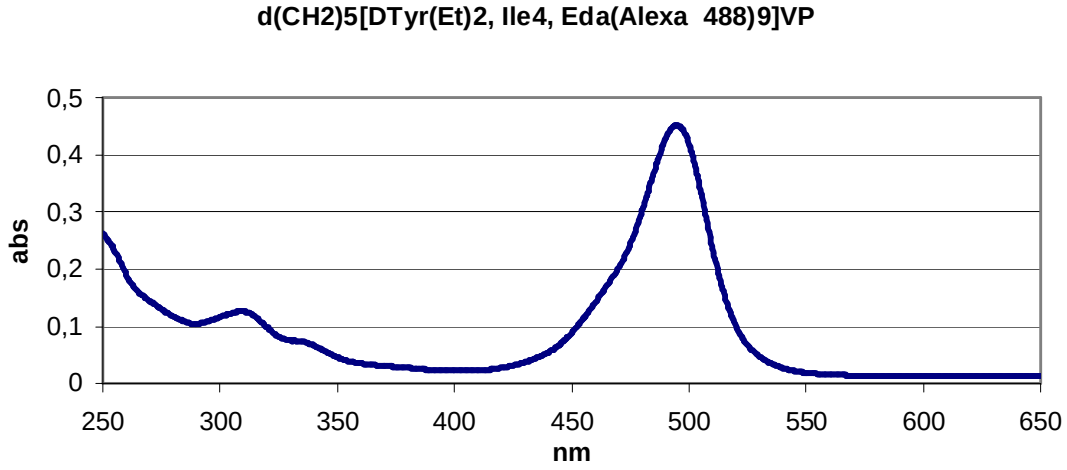

Supplementary Figure 35: Absorbance spectrum of d$(CH_2)_5$[DTyr(Et)^2, Ile^4, Eda(Alexa 488)^9]VP (**4**). Absorbance peak at 332 nm.

Nature Chemical Biology: doi: 10.1038/nchembio.396

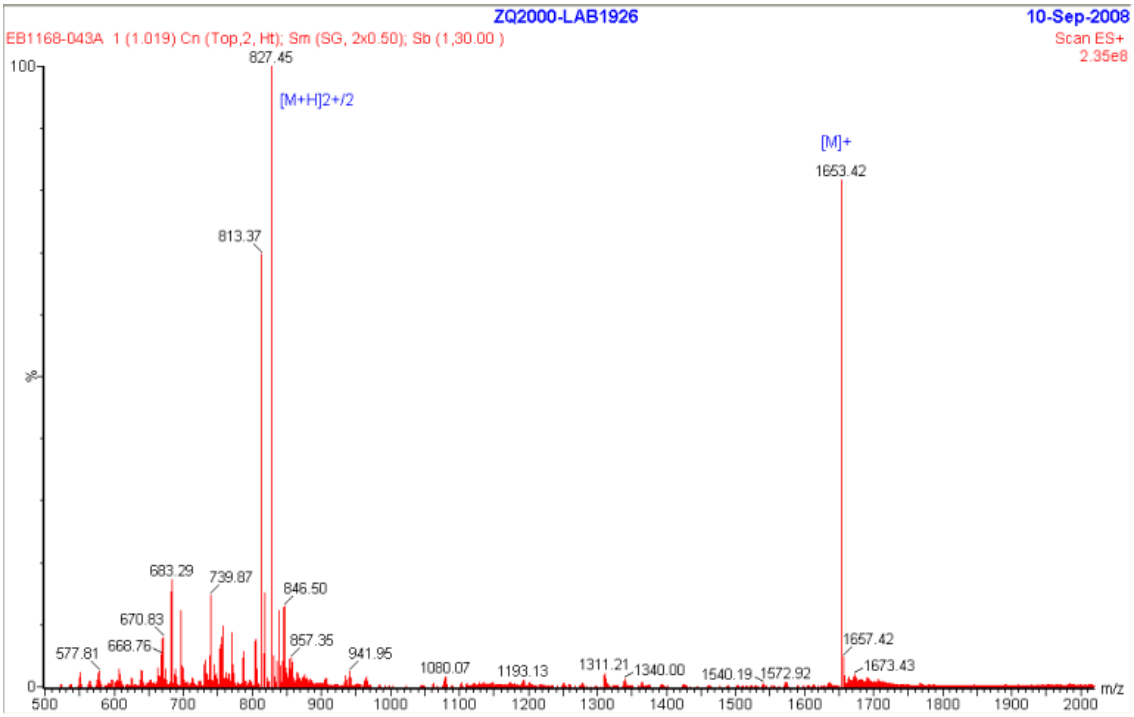

Supplementary Figure 36: Mass spectrometry characterization of d$(CH_2)_5$[DTyr(Et)^2, Ile^4, Eda(Alexa 488)^9]VP (**4**)

Nature Chemical Biology: doi: 10.1038/nchembio.396

Labeling of dopamine receptor antagonist, NAPS and agonist, PPHT.

NAPS-amine and PPHT-amine were synthesized as previously described [8]. Lumi4-Tb™-amine and d1-amine were purshased from CisBio Bioassays. NAPS-d1 is commercially available from CisBio Bioassays as Dopamine D_2 receptor red antagonist.

NAPS derivatives:

NAPS labeling with d1 and Lumi4-Tb™ fluorophore :

Since aromatic amine are poor nucleophic reagent, reaction between **NAPS**-amine and fluorophore-NHS failed. To circumvent this issue, we converted the ligand into corresponding NHS ester by reaction with glutaric anhydride followed by activation of carboxylic acid function with DCC-NHS method. In the second step this NHS ester ligand was condensed onto the corresponding dyes (Lumi4-Tb™-amine, d1-amine). Purification were performed by preparative HPLC and purified compounds were analysed by ES-MS (yielding Lumi4-Tb™ 35 % - d1 45 %).

NAPS-NH2 (**7**)

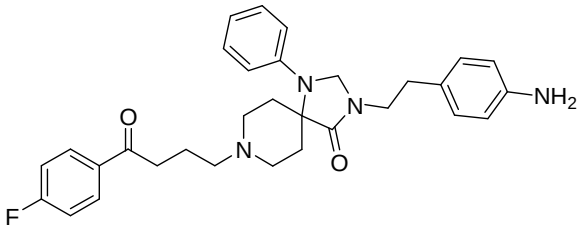

Nature Chemical Biology: doi: 10.1038/nchembio.396

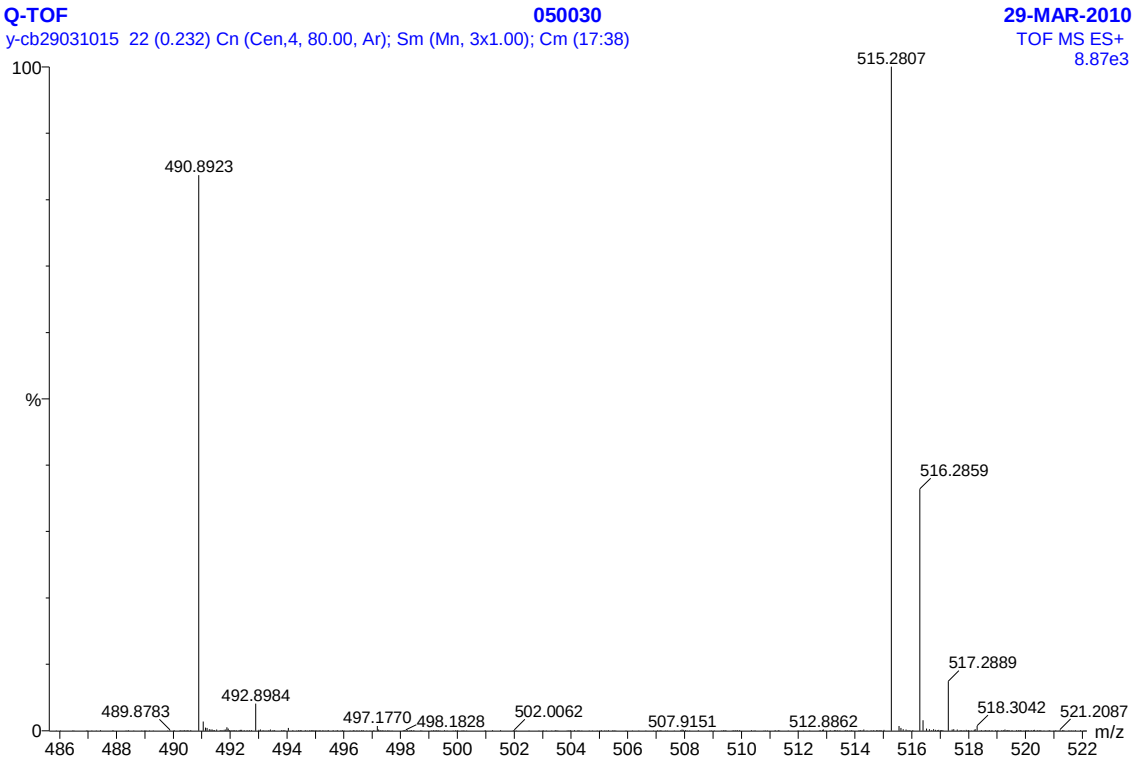

Supplementary Figure 37: Mass spectrometry characterization of NAPS-NH2 (**7**) *m/z* (HRMS^{+}) 515.2807 $[M+H]^{+}$ ($C_{31}H_{36}FN_4O_2$) Calcd 515.2817

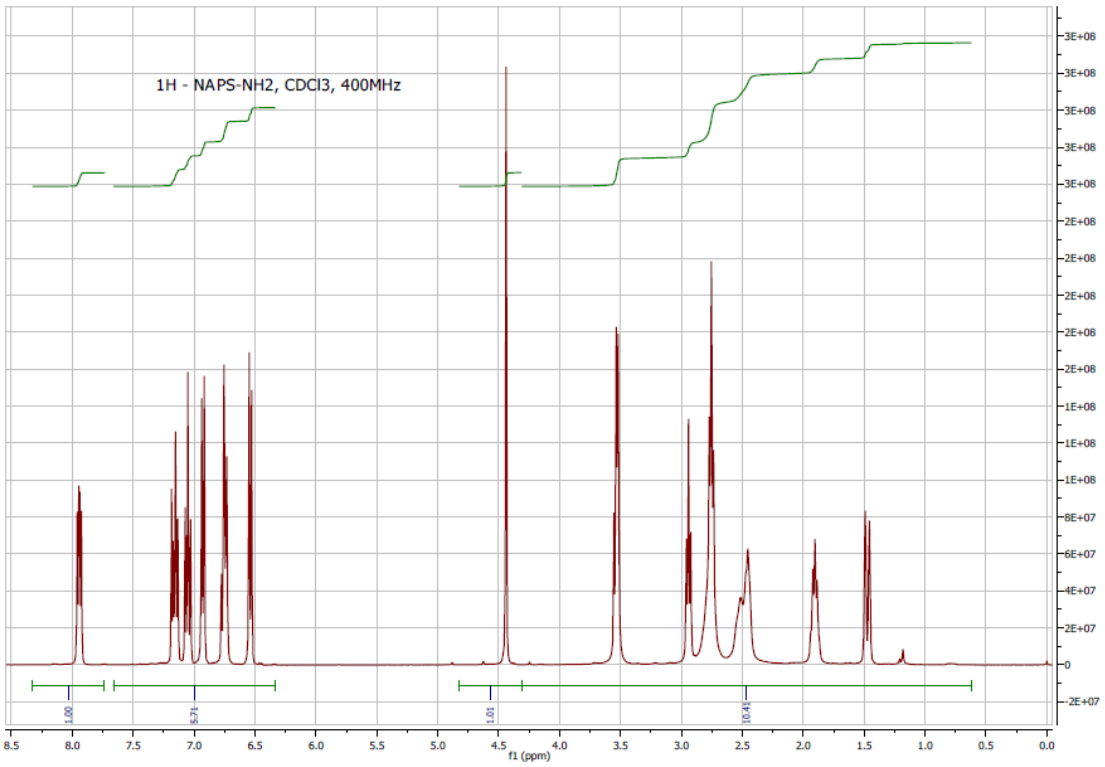

Supplementary Figure 38: 1H NMR spectrum of NAPS-NH_2 (**7**). NMR spectra have been recorded on Bruker AVANCE III NANO B - 400MHz using BBFO+ probe.

Nature Chemical Biology: doi: 10.1038/nchembio.396

^{1}H NMR ($CDCl_3$, 400 MHz) δ (ppm) : 7.94 (dd, 2H) ; 7.15 (t, 2H, J=7.9 Hz) ; 7.03 (t, 2H, J= 8.5 Hz) ; 6.93 (d, 2H, J=8.1 Hz) ; 6.73-6.78 (m, 3H) ; 6.54 (d, 2H, J= 8.1 Hz) ; 3.52-3.55 (m, 4H) ; 2.94 (t, 2H, J= 7.1 Hz) ; 2.74-2.77 (m, 12H), 2.45-2.51 (m, 4H) ; 1.89-1.92 (m, 2H) ; 1.47 (d, 2H, J= 13.8 Hz).

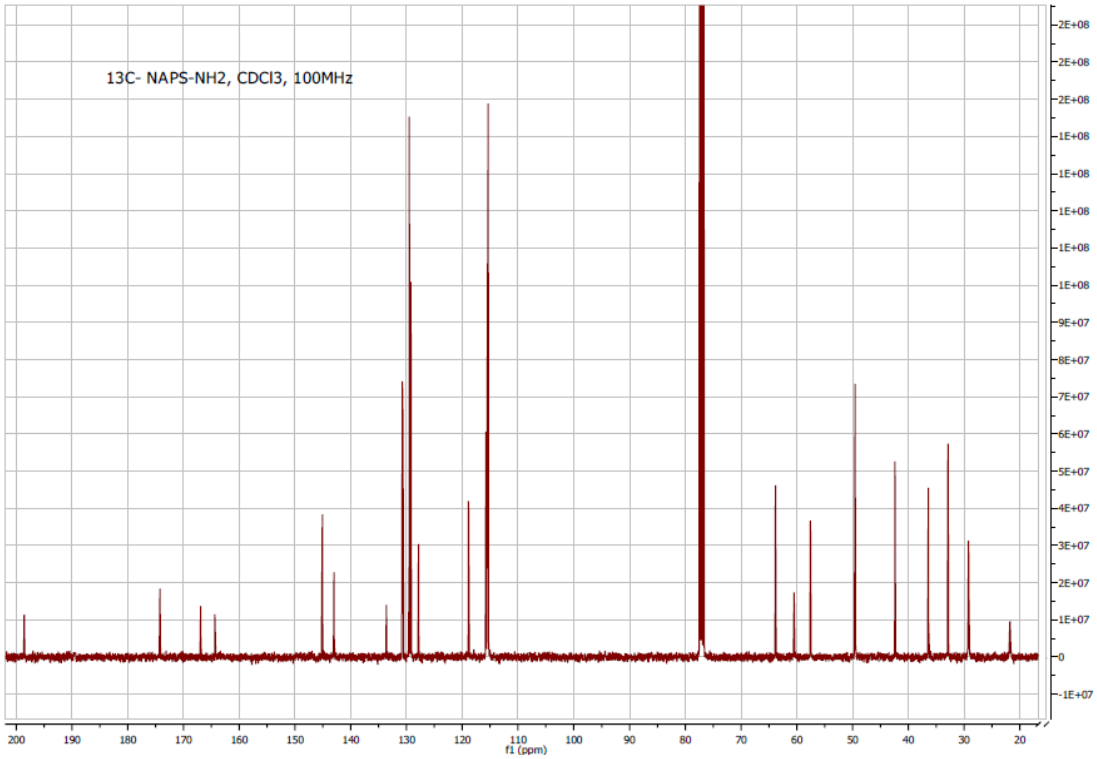

Supplementary Figure 39: 13C NMR spectrum of NAPS-NH_2 (**7**). NMR spectra have been recorded on Bruker AVANCE III NANO B - 400MHz using BBFO+ probe.

^{13}C ($CDCl_3$, 100 MHz) δ (ppm) : 198.57, 174.24, 166.91, 164.38, 145.09, 143.01, 133.64, 133.61, 130.74, 130.65, 129.51, 129.21, 127.84, 118.88, 115.74, 115.52, 115.42, 115.35, 63.81, 60.47, 57.55, 49.54, 42.38, 36.39, 32.88, 29.18, 21.75.

Nature Chemical Biology: doi: 10.1038/nchembio.396

NAPS-Glu-CO_2H:

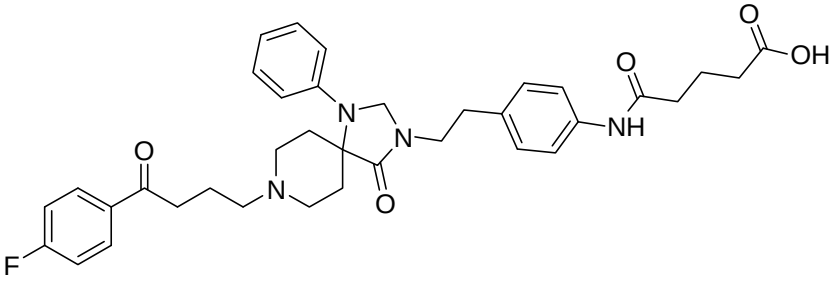

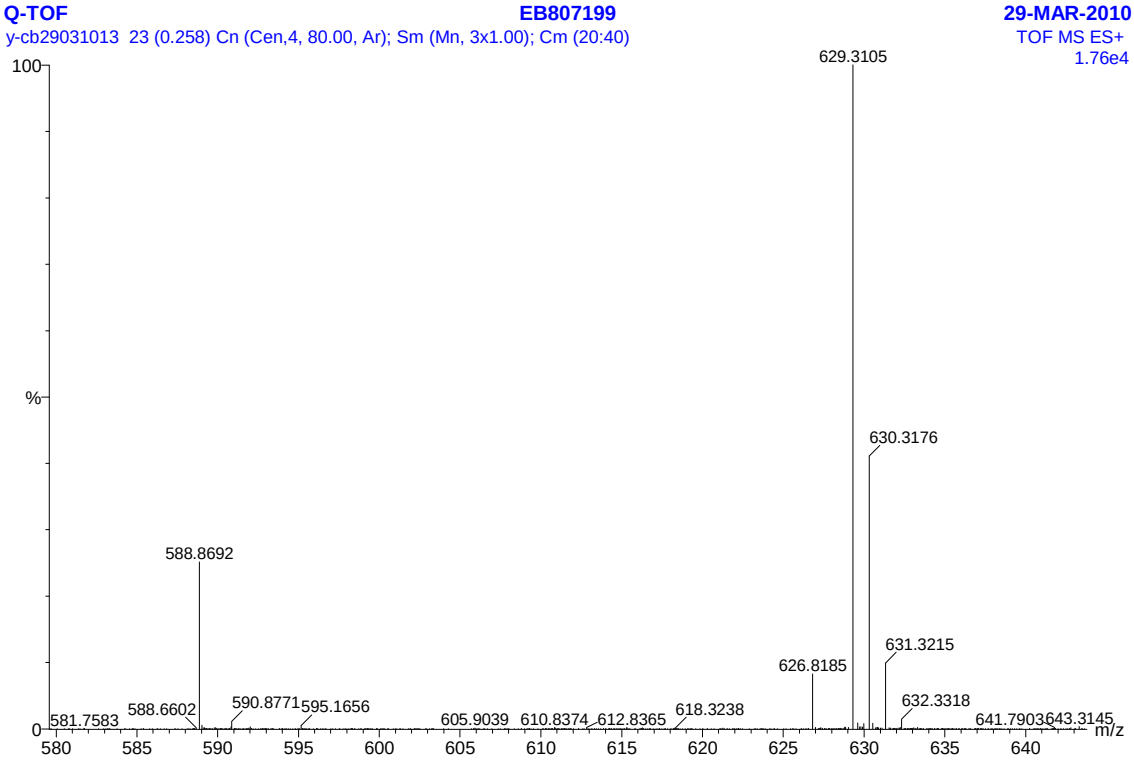

Supplementary Figure 40: Mass spectrum of NAPS-Glu-CO_2H. *m/z* ($HRMS^+$) 629.3105 $[M+H]^+$ ($C_{36}H_{42}FN_4O_5$) Calcd 629.3134

Nature Chemical Biology: doi: 10.1038/nchembio.396

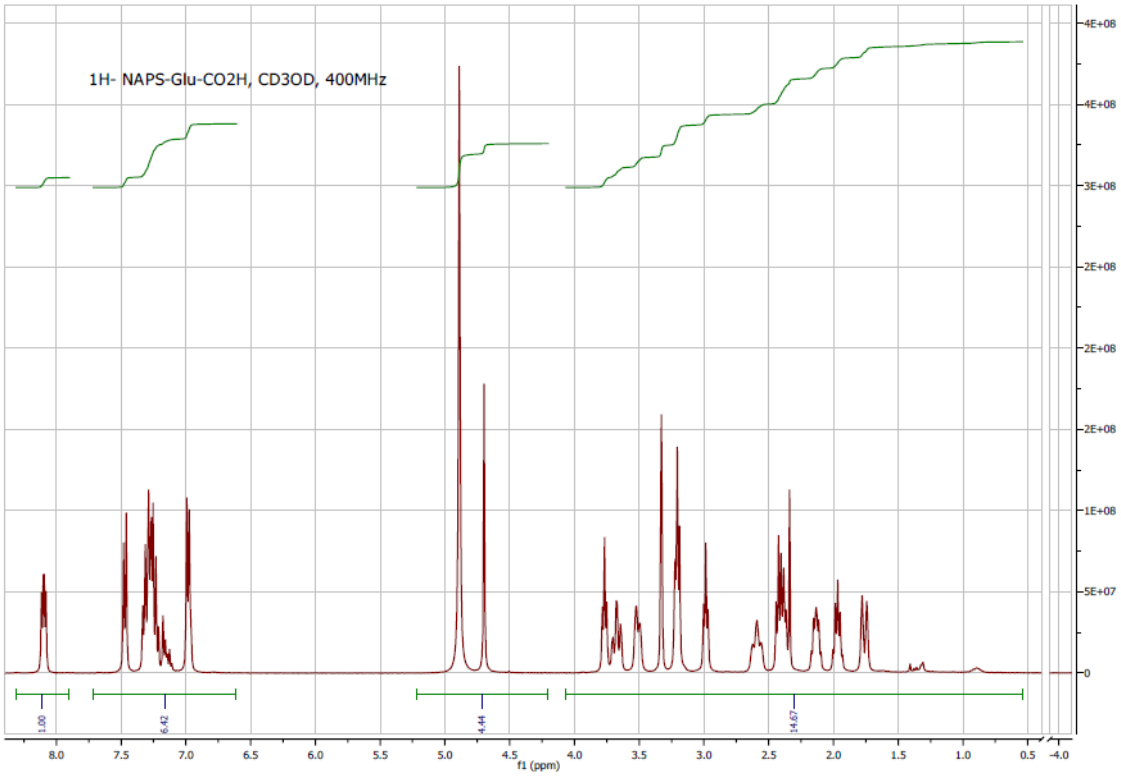

Supplementary Figure 41: 1H NMR of NAPS-Glu-CO_2H. NMR spectra have been recorded on Bruker AVANCE III NANO B - 400MHz using BBFO+ probe.

^{1}H NMR (CD_3OD, 400 MHz) δ (ppm) : 8.09 (dd, 2H); 7.47 (d, 2H, J= 8.3 Hz); 7.21-7.33 (m, 7H); 6.98 (d, 2H, J= 7.5 Hz); 3.77 (t, 2H, J= 6.7 Hz); 3.68 (t, 2H, J= 12.7 Hz), 3.51 (d, 2H, J= 10.6 Hz) ; 3.19-3.22 (m, 4H) ; 2.99 (t, 2H, J=6.7 Hz) ; 2.59 (t, 2H, J= 13.1 Hz) ; 2.37-2.44 (m, 4H) ; 2.34 (s, 1H) ; 2.10-2.15 (m, 2H) ; 1.95-2.00 (m, 2H) ; 1.76 (d, 2H, J= 14.8 Hz).

Nature Chemical Biology: doi: 10.1038/nchembio.396

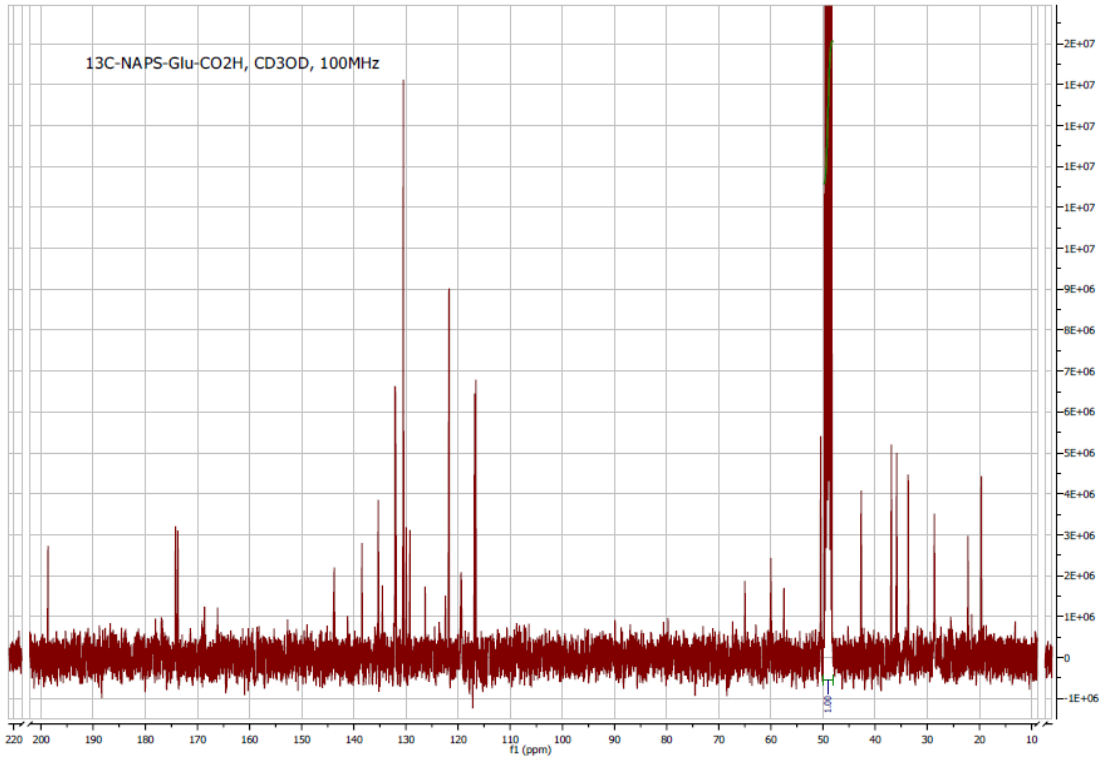

Supplementary Figure 42: 13C NMR of NAPS-Glu-CO_2H. NMR spectra have been recorded on Bruker AVANCE III NANO B - 400MHz using BBFO+ probe.

^{13}C (CD_3OD, 100 MHz) δ (ppm) :.198.66, 174.21, 173.76, 143.75, 138.45, 135.32, 132.09, 132.00, 130.54, 130.50, 129.94, 129.23, 121.73, 116.82, 116.60, 60.01, 50.45, 42.68, 36.87, 35.87, 33.67, 28.65, 22.20, 19.64.

Nature Chemical Biology: doi: 10.1038/nchembio.396

NAPS(Lumi4-Tb) (8) :

Acquired: 16/02/2009 10:35:16
Printed: 16/02/2009 11:06:30

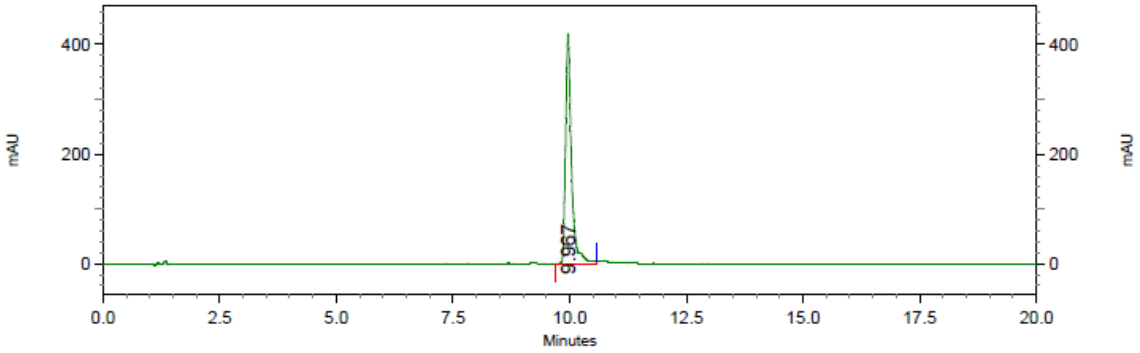

UV2000-337nm
Results (eb
(16/02/2009
11:06:19)
(Reprocessed))

Retention Time	Area	Area %	Height	Height %
9.967	3684451	100.00	419721	100.00
Totals	3684451	100.00	419721	100.00

Supplementary Figure 43: HPLC spectrum of NAPS(Lumi4-Tb) (**8**)

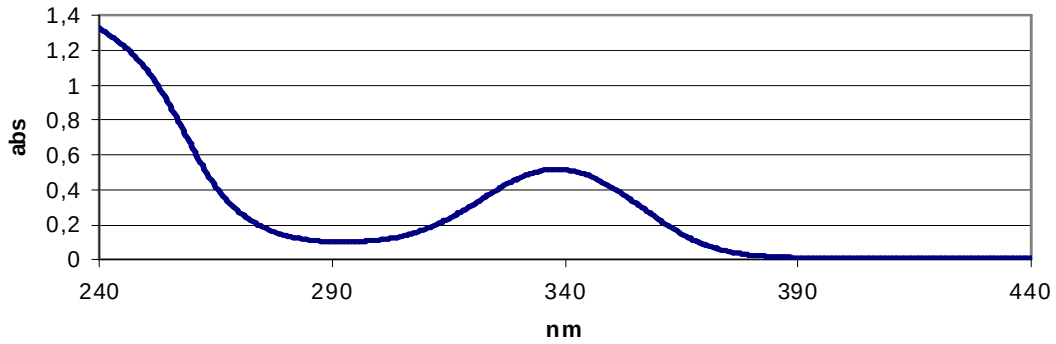

Supplementary Figure 44: Absorbance spectrum of NAPS(Lumi4-Tb) (**8**) . Absorbance peak at 339 nm.

Nature Chemical Biology: doi: 10.1038/nchembio.396

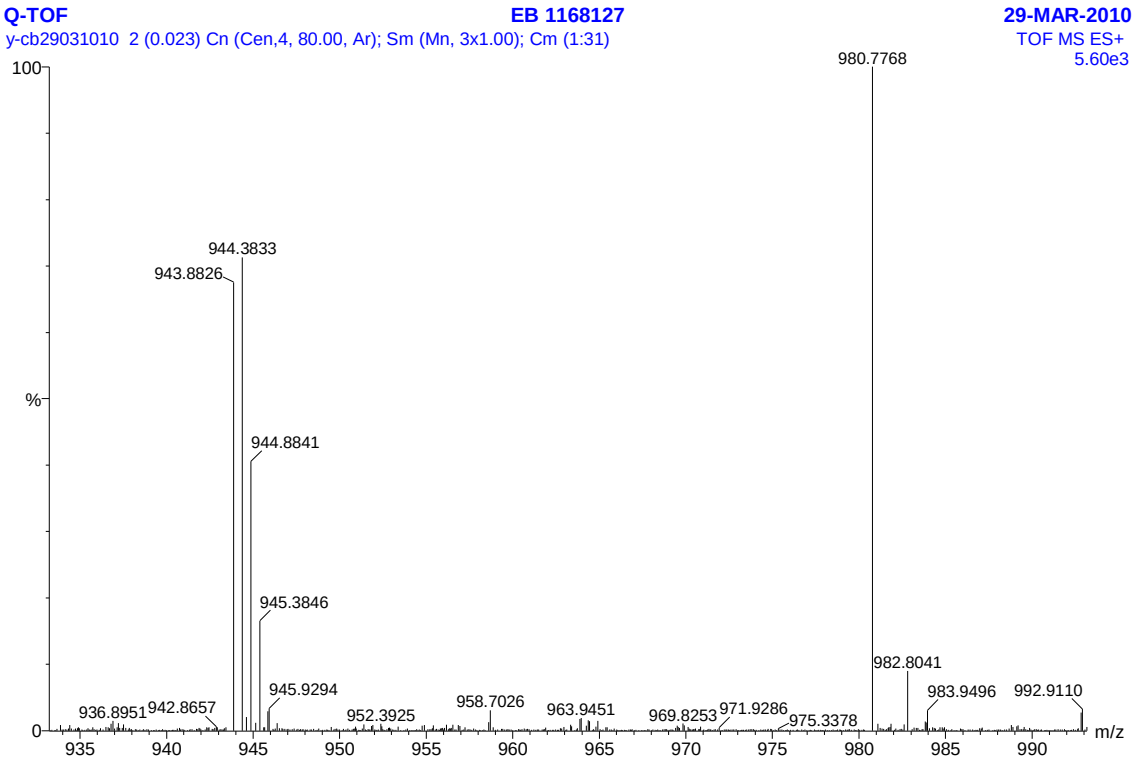

Supplementary Figure 45: Mass spectrometry characterization of NAPS(Lumi4-Tb) (**8**). *m/z* (HRMS$^+$) 943.8826 $[M]^+/2$ ($C_{92}H_{111}FN_{17}O_{16}Tb$) Calcd 943.8810

Nature Chemical Biology: doi: 10.1038/nchembio.396

NAPS(d1) (9):

Acquired: 10/02/2009 14:30:07
Printed: 13/02/2009 13:25:07

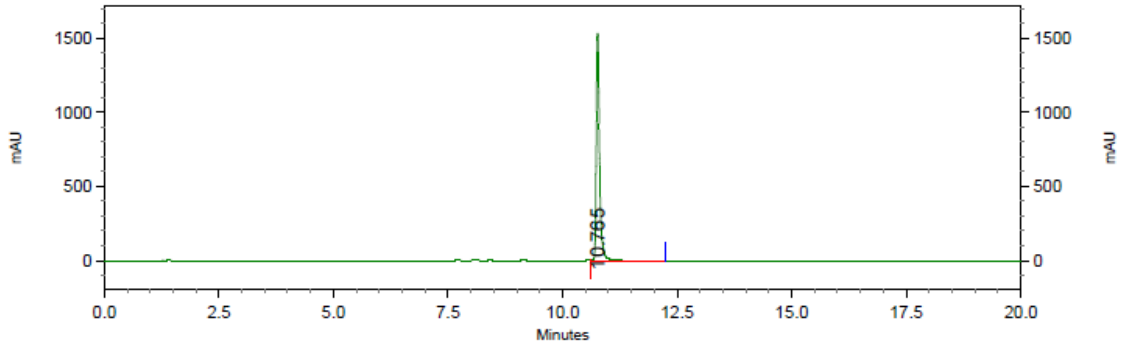

UV2000-650nm Results (eb (10/02/2009 15:00:20) (Original))

Retention Time	Area	Area %	Height	Height %
10.765	7636230	100.00	1534674	100.00
Totals	7636230	100.00	1534674	100.00

Supplementary Figure 46: HPLC spectrum of NAPS(d1) (**9**)

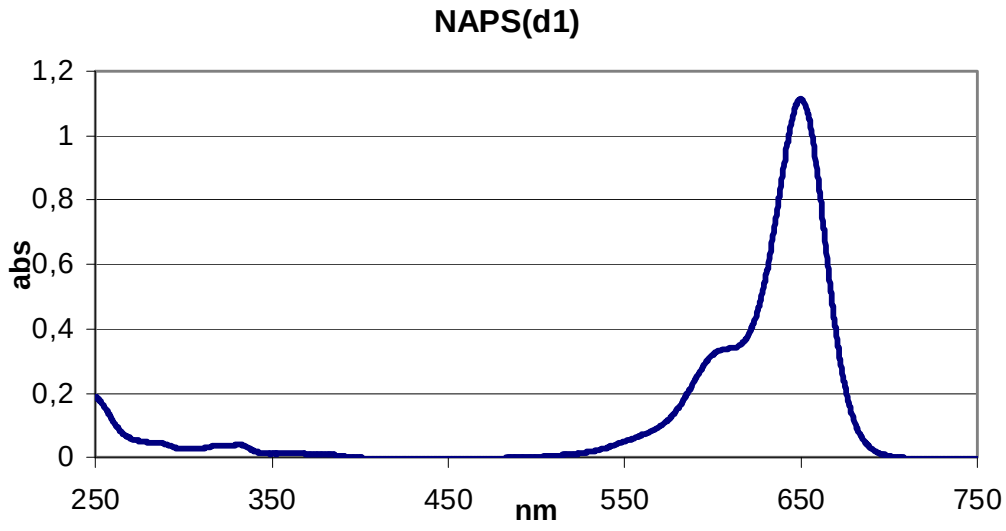

Supplementary Figure 47: Absorbance spectrum of NAPS(d1) (**9**) . Absorbance peak at 650 nm.

Nature Chemical Biology: doi: 10.1038/nchembio.396

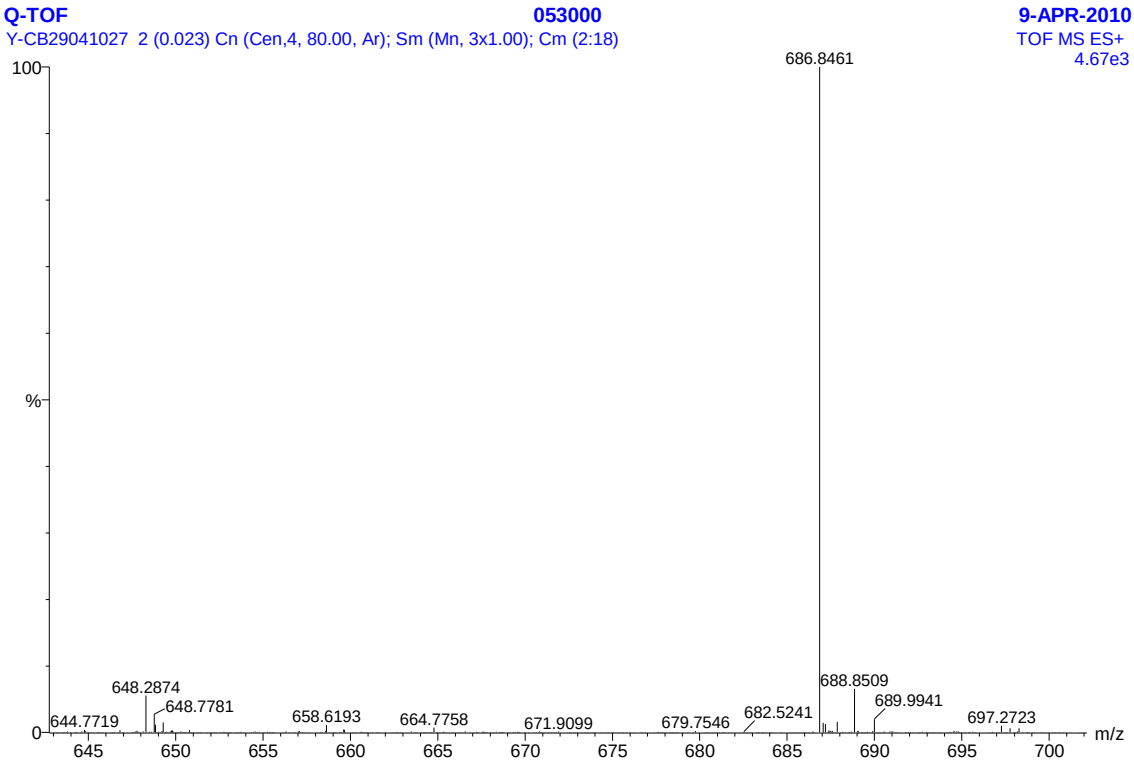

Supplementary Figure 48: Mass spectrometry characterization of NAPS(d1) (**9**). *m/z* (HRMS$^+$) 686.8461 $[M]^+$/2+K ($C_{31}H_{36}FN_4O_2$) Calcd 686.7477

Nature Chemical Biology: doi: 10.1038/nchembio.396

PPHT derivatives:

PPHT labeling with d1 and Lumi4-Tb™ fluorophore :

Since aromatic amine are poor nucleophic reagent, reaction between PPHT-amine and fluorophore-NHS failed. As for NAPS-amine, we converted the ligand into corresponding NHS ester by reaction with glutaric anhydride followed by activation of carboxylic acid function with DCC-NHS method. In the second step this NHS ester ligand was condensed onto the corresponding dyes (Lumi4-Tb™-amine, d1-amine). Purification were performed by preparative HPLC and purified compounds were analyzed by ES-MS (yielding 40%).

PPHT-NH_2 (10)

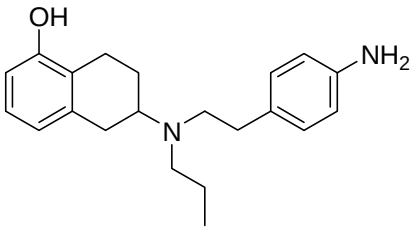

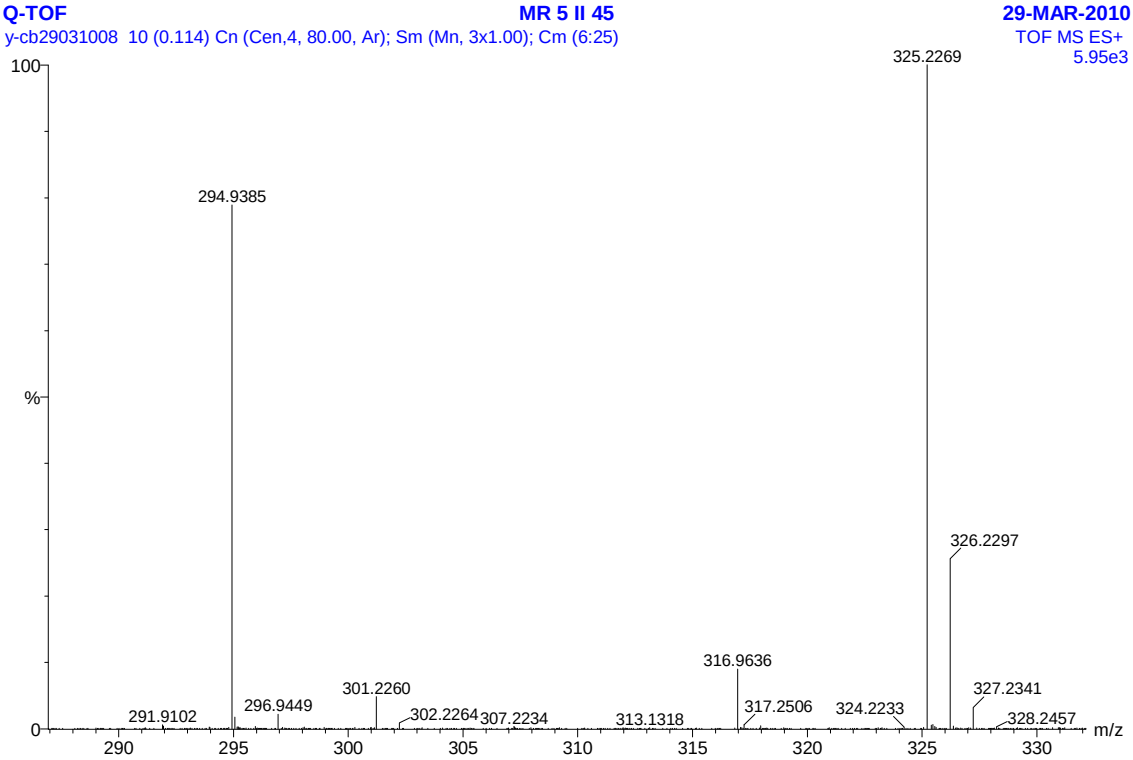

Supplementary Figure 49: Mass spectrometry characterization of PPHT-NH_2 (**10**). *m/z* (HRMS$^+$) 325.2269 $[M+H]^+$ ($C_{21}H_{29}N_2O$) Calcd 325.2274

Nature Chemical Biology: doi: 10.1038/nchembio.396

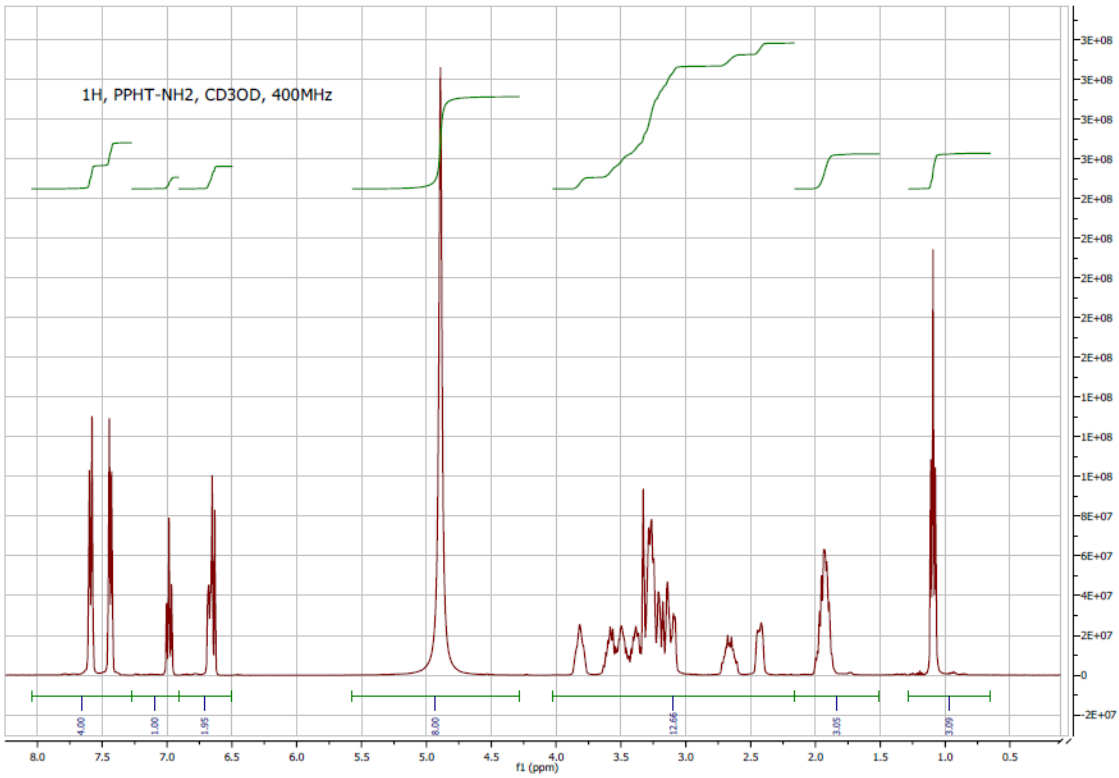

Supplementary Figure 50: 1H NMR of PPHT-NH_2 (**10**). NMR spectra have been recorded on Bruker AVANCE III NANO B - 400MHz using BBFO+ probe.

^{1}H NMR (CD_3OD, 400 MHz) δ (ppm) . 7.79 (d, 2H, J= 7.8 Hz); 7.44 (d, 2H, J= 7.2 Hz) ; 6.98 (t, 1H, J= 7.8 Hz) ; 6.63-6.68 (m, 2H) ; 3.81-3.84 (m, 1H) ; 3.10-3.62 (m, 10H) ; 2.63-2.70 (m, 1H) ; 2.41-2.43 (m, 1H) ; 1.89-1.98 (m, 3H) ; 1.09 (t, 3H, J= 7.2 Hz).

Nature Chemical Biology: doi: 10.1038/nchembio.396

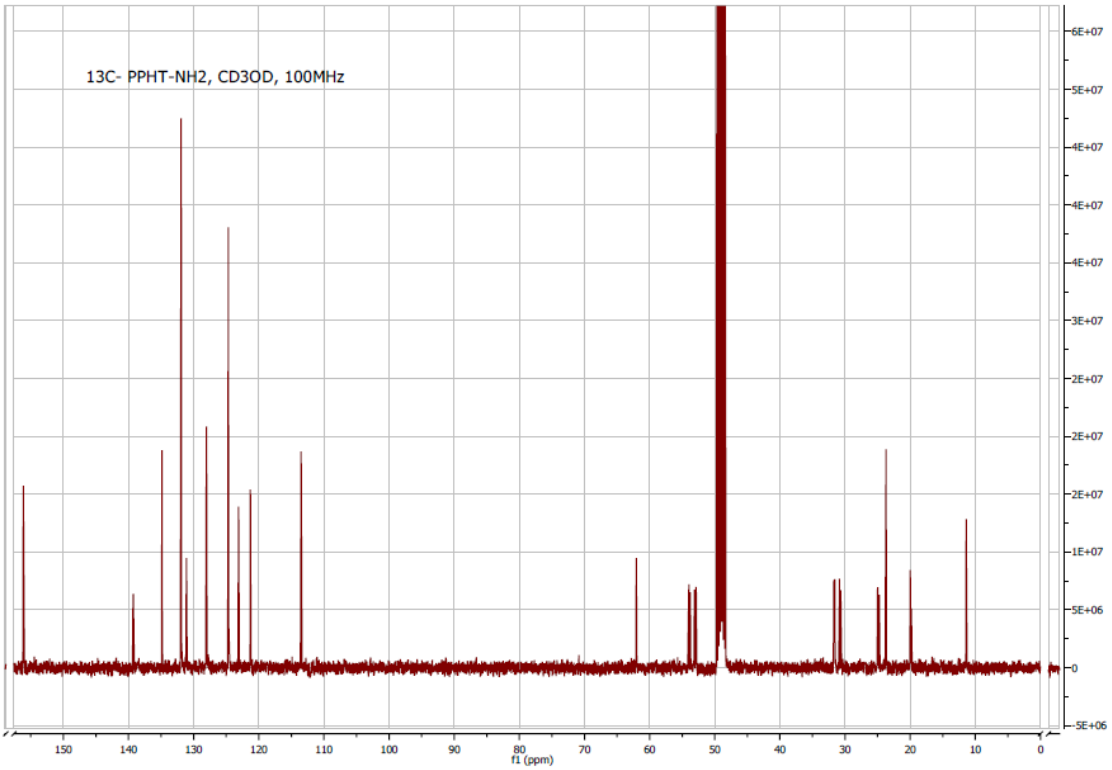

Supplementary Figure 51: 13C NMR of PPHT-NH_2 (**10**). NMR spectra have been recorded on Bruker AVANCE III NANO B - 400MHz using BBFO+ probe.

^{13}C (CD_3OD, 100 MHz) δ (ppm) :156.14, 139.29, 139.25, 134.84, 131.91, 131.09, 128.02, 124.66, 123.10, 121.29, 113.50, 62.05, 53.97, 53.75, 53.13, 52.87, 31.72, 31.57, 30.85, 30.67, 25.00, 24.75, 23.72, 19.99, 19.83, 11.40.

Nature Chemical Biology: doi: 10.1038/nchembio.396

PPHT-Glu-CO_2H

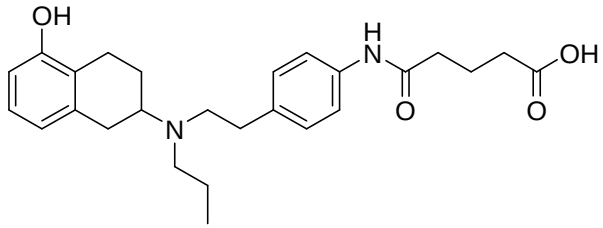

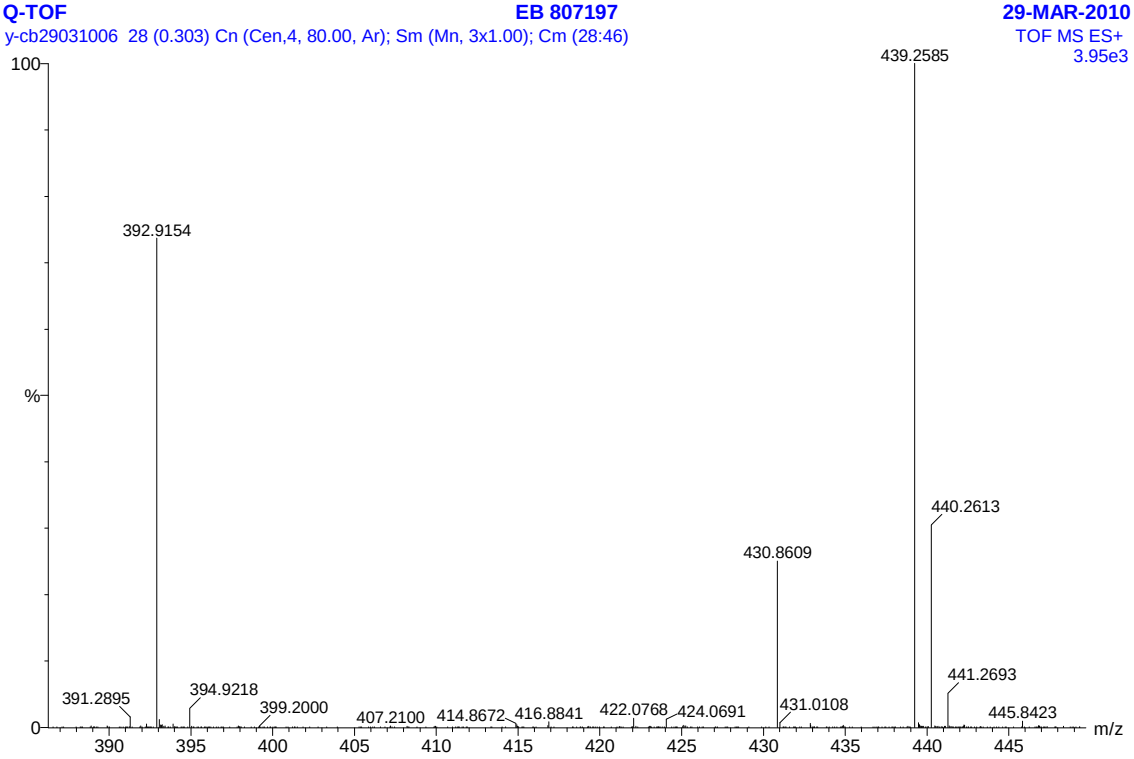

Supplementary Figure 52: Mass spectrometry characterization of PPHT-Glu-CO_2H. *m/z* (HRMS$^+$) 439.2585 $[M+H]^+$ ($C_{26}H_{35}N_2O_4$) Calcd 439.2591

Nature Chemical Biology: doi: 10.1038/nchembio.396

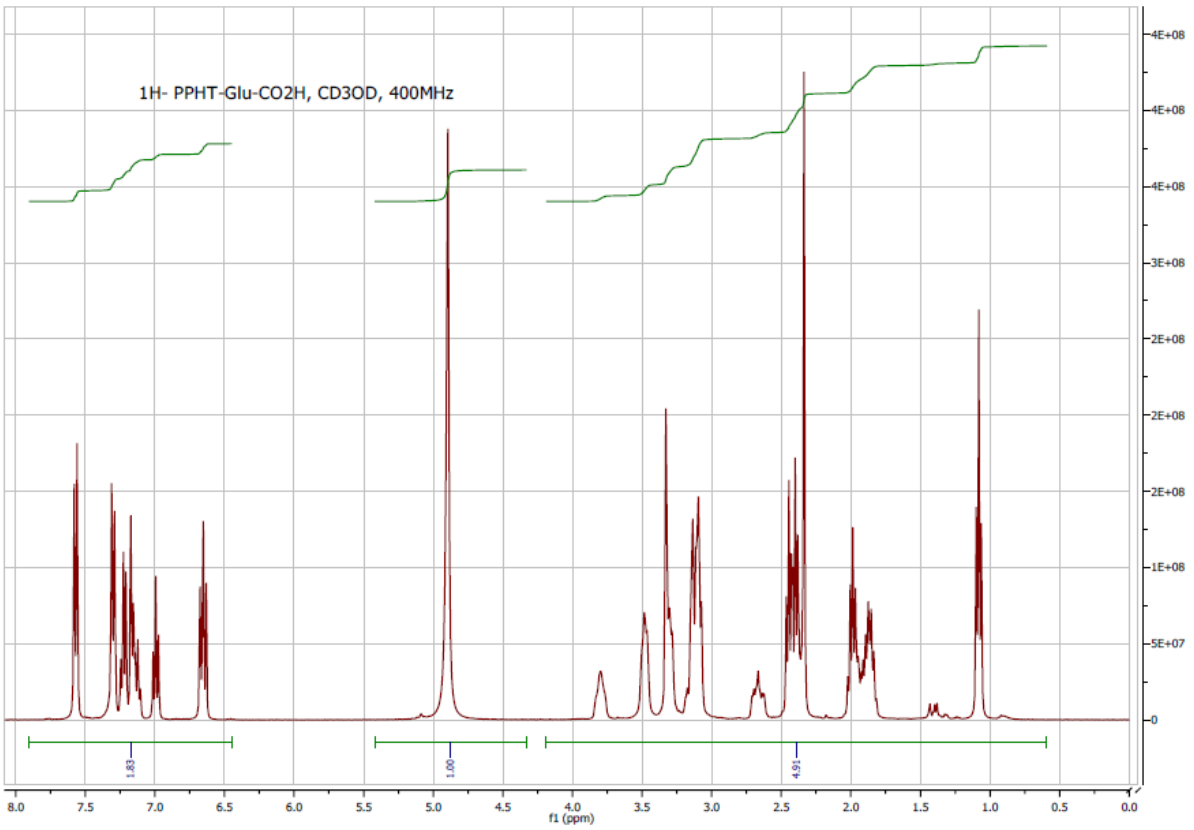

Supplementary Figure 53: 1H NMR of PPHT-Glu-CO_2H. NMR spectra have been recorded on Bruker AVANCE III NANO B - 400MHz using BBFO+ probe.

^{1}H NMR (CD_3OD, 400 MHz) δ (ppm) : 7.57 (d, 2H, J= 8.3Hz); 7.30 (d, 2H, J= 8.3 Hz); 7.12-7.23 (m, 4H); 6.99 (t, 1H, J= 7.8 Hz); 6.65 (t, 1H, J= 8.4 Hz); 3.78-3.81 (m, 1H); 3.45-3.50 (m, 2H); 3.29-3.34 (m, 3H), 3.07-3.16 (m, 5H); 2.65-2.70 (m, 1H); 2.30-2.47 (m, 4H); 1.83-2.02 (m, 5H); 108 (t, 3H, J= 7.3 Hz).

Nature Chemical Biology: doi: 10.1038/nchembio.396

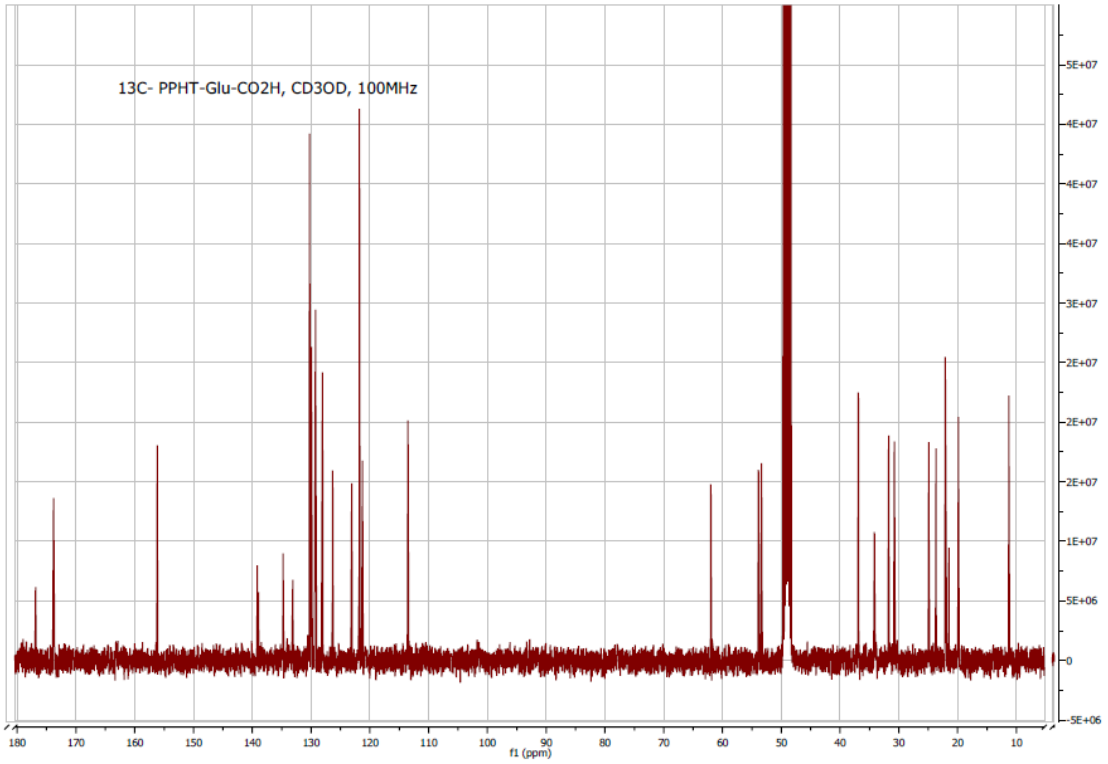

Supplementary Figure 54: 13C NMR of PPHT-Glu-CO_2H. NMR spectra have been recorded on Bruker AVANCE III NANO B - 400MHz using BBFO+ probe.

^{13}C (CD_3OD, 100 MHz) δ (ppm) :176.87, 173.81, 156.16, 139.16, 138.94, 134.76, 133.11, 130.27, 129.23, 128.06, 126.32, 123.07, 121.77, 121.26, 113.51, 61.99, 53.89, 53.35, 36.89, 34.16, 31.74, 30.77, 24.91, 23.68, 21.49, 19.85, 11.30.

Nature Chemical Biology: doi: 10.1038/nchembio.396

PPHT(Lumi4-Tb) (11) :

Acquired: 16/02/2009 11:50:00
Printed: 16/02/2009 13:00:37

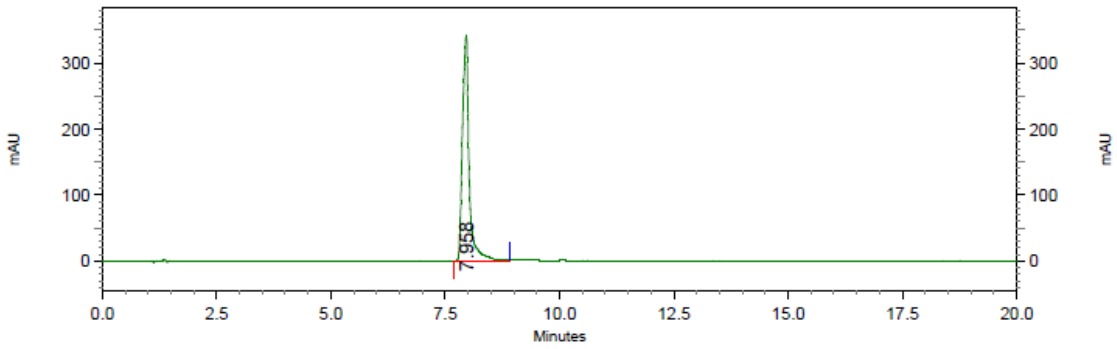

UV2000-337nm
Results (eb
(16/02/2009
13:00:08)
(Reprocessed))

Retention Time	Area	Area %	Height	Height %
7.958	3500239	100.00	342018	100.00
Totals	3500239	100.00	342018	100.00

Supplementary Figure 55: HPLC spectrum of PPHT(Lumi4-Tb) (**11**)

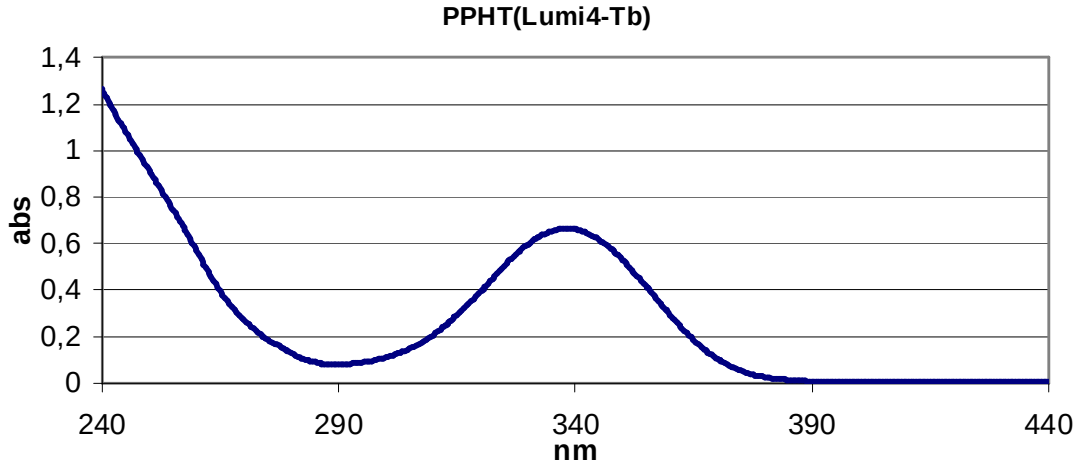

Supplementary Figure 56: Absorbance spectrum of PPHT(Lumi4-Tb) (**11**) . Absorbance peak at 338 nm.

Nature Chemical Biology: doi: 10.1038/nchembio.396

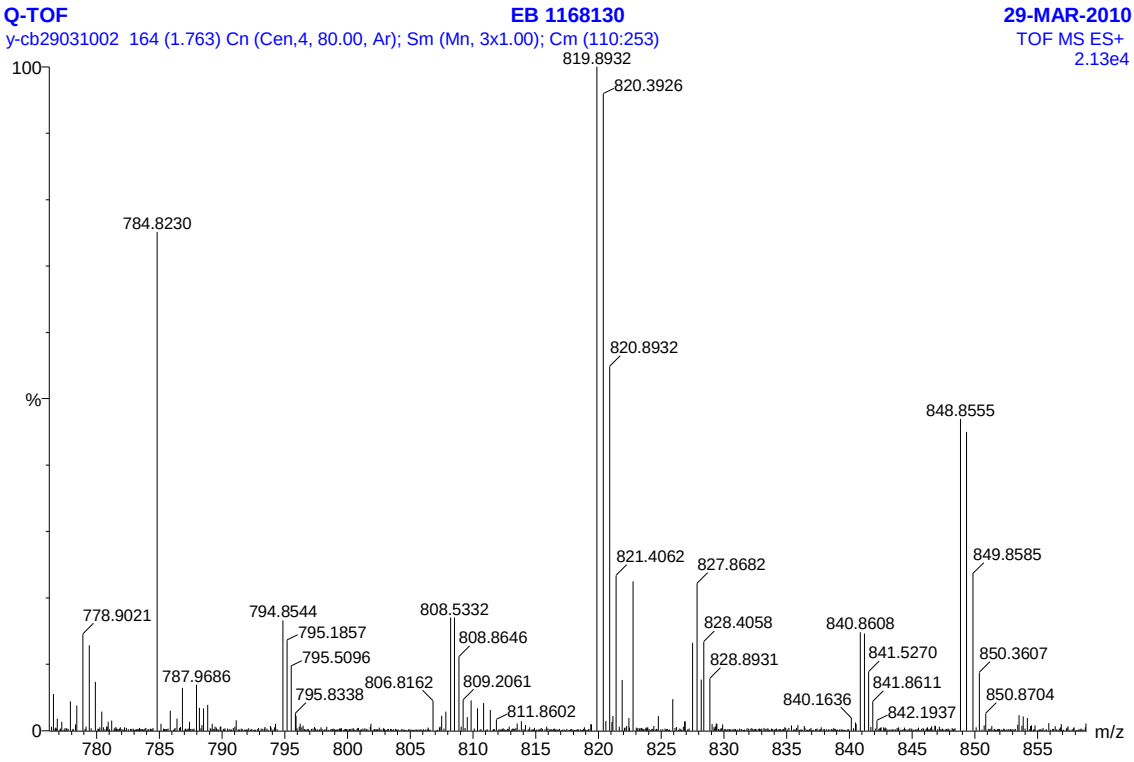

Supplementary Figure 57: Mass spectrometry characterization of PPHT(lumi4-Tb) (**11**). *m/z* (HRMS$^+$) 848.8555 $[M+H]^+/2$ ($C_{82}H_{104}N_{15}O_{15}Tb$) Calcd 848.8539

Nature Chemical Biology: doi: 10.1038/nchembio.396

PPHT(d1) (12) :

Acquired: 10/02/2009 15:07:02
Printed: 13/02/2009 13:25:42

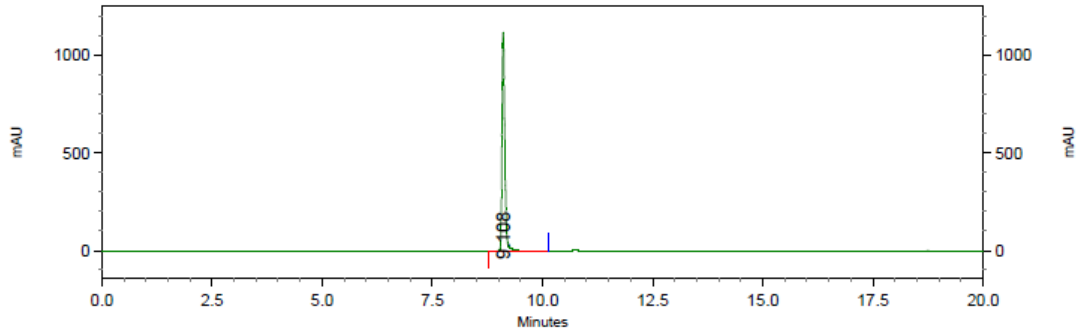

UV2000-650nm
Results (eb
(10/02/2009
15:37:01)
(Original))

Retention Time	Area	Area %	Height	Height %
9.108	4888188	100.00	1117099	100.00
Totals	4888188	100.00	1117099	100.00

Supplementary Figure 58: HPLC spectrum of PPHT(d1) (**12**)

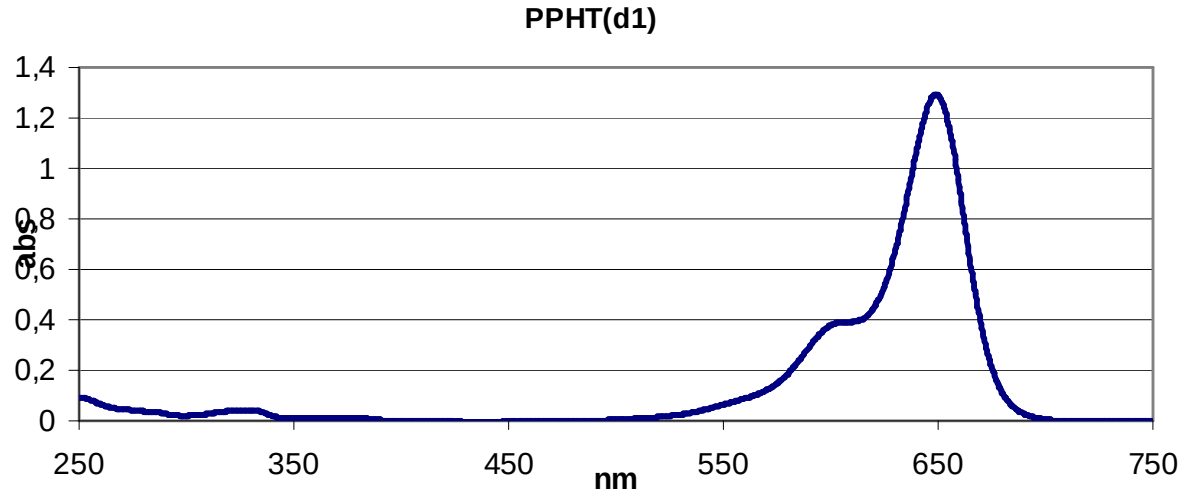

Supplementary Figure 59: Absorbance spectrum of PPHT(d1) (**12**) . Absorbance peak at 649 nm.

Nature Chemical Biology: doi: 10.1038/nchembio.396

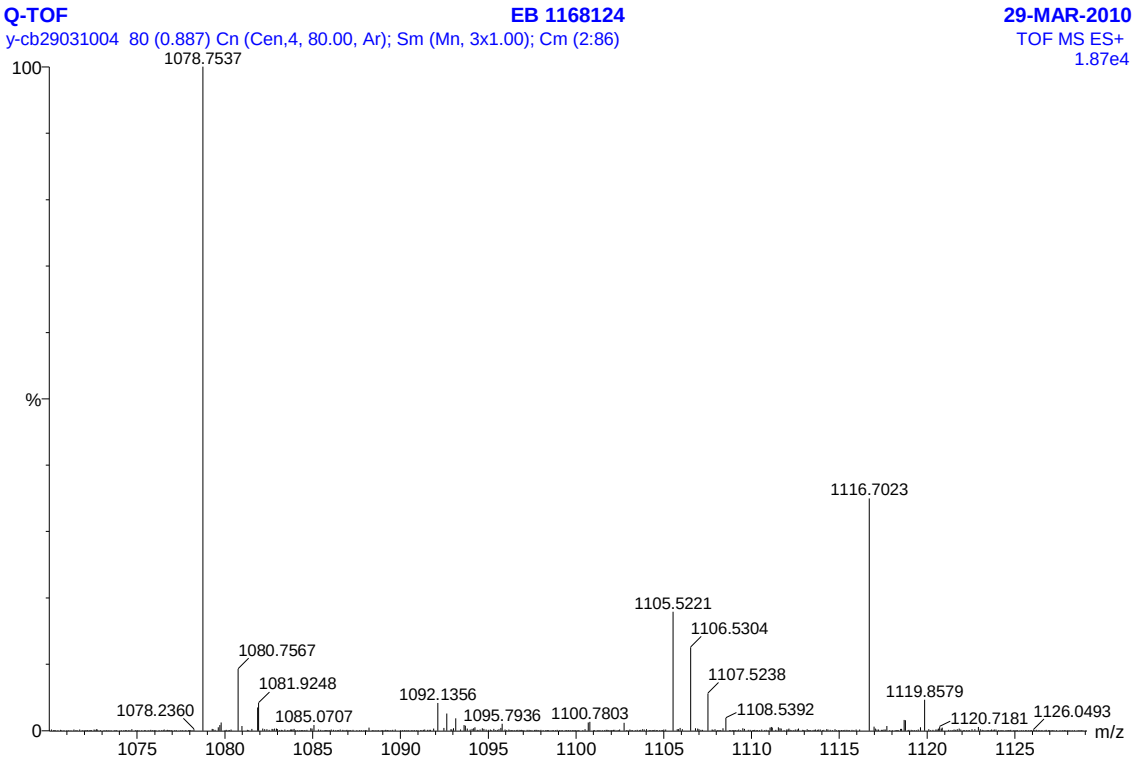

Supplementary Figure 60: Mass spectrometry characterization of PPHT(d1) (**12**). *m/z* (HRMS$^+$) 1105.5221 $[M+H]^+$ ($C_{60}H_{77}N_6O_{10}S_2$) Calcd 1105.5137

Nature Chemical Biology: doi: 10.1038/nchembio.396

Cell Culture

The CHO cell lines stably expressing the human vasopressin V_{1a}, or oxytocin receptors and the Cos7 cell lines were maintained in culture in Dulbecco's modified Eagle's medium supplemented with 10% fetal calf serum and 100 units/ml penicillin and streptomycin in an atmosphere of 95% air and 5% CO_2 at 37°C. The expression levels of the V_{1a} and OT receptors by the CHO cells were respectively in the range of 0.7-2 pmole/mg protein and 0.3-0.7 pmole/mg protein, depending on the confluence of the cells and the number of cell passages.

Cos7 cells were transiently transfected by electroporation as previously described [9] with 1 µg of vector coding for the V_{1a} or oxytocin receptor and empty vector to a final amount of 10 µg. Under these conditions, the expression level was in the range of 0.5 to 2 pmole/mg protein.

Membrane Preparations

Culture dishes of Cos7 or CHO cells expressing the human vasopressin V_{1a} or oxytocin receptors were washed twice in PBS without calcium and magnesium, and cold lysis buffer (15 mM Tris:HCl, 2 mM $MgCl_2$, 0.3 mM EDTA, pH 7.4) was added. Cells were scraped with a rubber policeman, homogenized with a Ultra-Turrax homogenizer (Janke-Kunkel IKA-Labortechnik, Staufen, Germany), and centrifuged at 100g for 5 min at 4°C. Supernatants were recovered and centrifuged at 44,000g for 30 min at 4°C. Pellets were resuspended in a suspension medium (50 mM Tris:HCl, 5 mM $MgCl_2$, pH 7.4) and centrifuged at 44,000g for 30 min at 4°C. Pellets were resuspended in an appropriate volume of the same buffer. For each membrane preparation, the protein content was evaluated and the membranes were then aliquoted and frozen in liquid nitrogen.

Membranes from mammary glands were prepared as previously described [10]. Briefly, mammary glands were obtained from 3-week lactating rats. The dissected mammary gland was free of fascia and connective tissue and homogenized in ice-cold 10 mM Tris HCl (pH 7.4), 1 mM EDTA, and 300 mM KCl buffer with Polytron at setting six for three periods of 10 seconds each. The homogenate was centrifuged for 10 min at 1,000g. The resulting supernatant was centrifuged for 30 min at 12,000g. The pellet was washed in 10 mM Tris HCl (pH 7.4) and 1 mM EDTA and then resuspended in 15 ml 10% sucrose (wt/vol), 10 mM Tris HCl (pH 7.4), and 1 mM EDTA which was layered onto 15 ml 35% sucrose (wt/vol), 10 mM Tris HCl (pH 7.4), and 1 mM EDTA. After centrifugation for 2 h at 100,000g (Beckman ultracentrifuge), the membranes were collected at the 10-35% interface. The membranes were

Nature Chemical Biology: doi: 10.1038/nchembio.396

dispersed in 50 mM Tris HCl (pH 7.4), 10 mM $MgCl_2$, washed, and resuspended in the same medium. The expression level of the mammary glands expressing oxytocin receptors was in the range of 0.5 to 4 pmole/mg protein.

Human fetal annexe tissues were cut into small pieces in lysis buffer (Tris 15 mM, $MgCl_2$, 2 mM, EDTA 0.3 mM) and homogenized with a Ultra-Turrax homogenizer (Janke-Kunkel IKA-Labortechnik, Staufen, Germany) for 45 seconds. The preparation was centrifuged at 100g for 5 min at 4°C to remove large fragments. Supernatants were recovered and centrifuged at 44,000g for 30 min at 4°C. Pellets were resuspended in a suspension medium (50 mM Tris:HCl, 5 mM $MgCl_2$, pH 7.4) and centrifuged at 44,000g for 30 min at 4°C. Pellets were resuspended in an appropriate volume of the same buffer. The expression level of the fetal annexes expressing oxytocin/vasopressin receptors was in the range of 20 to 100 fmole/mg protein.

Radioligand Binding Assays

Competition experiments were performed on membranes from CHO cells expressing human vasopressin V_{1a}, or oxytocin receptors, as previously described [11]. Briefly, membranes were incubated for 1 h at 30°C with [^{3}H]AVP (1-2 nM) and with increasing concentrations of fluorescent agonists ranging from 1 pM to 1 µM. Nonspecific binding was determined with an excess of AVP (1 µM). Bound tritiated vasopressin ([^{3}H]AVP) fractions were separated from the free tritiated vasopressin by filtration. We used Whatman GF-C filters (Whatman, Maidstone, UK) preincubated in bovine serum albumin (10 mg/ml). Filtration was performed on a Brandel apparatus (Brandel Inc., Gaithersburg, MD). Radioactivity on the filters was counted on a beta-counter Tri-carb 2100TR (PerkinElmer Life and Analytical Sciences). Each assay was performed in triplicate. All binding data were analyzed with the program Graphpad Prism.

The affinity of [^{3}H]OT was determined from saturation experiments on mammary gland membranes expressing OT receptors. Mammary gland membranes (7-15 µg/assay) were incubated with [^{3}H]OT (1-2 nM) plus increasing concentrations of OT (1 pM to 1 µM). Nonspecific binding was determined by the addition of a large excess of OT (1 µM). Bound and free ligand fractions were separated by filtration as mentioned above. Each assay was performed in triplicate. Radioactivity was counted on a beta-counter Tri-carb 2100TR (PerkinElmer Life and Analytical Sciences).

Nature Chemical Biology: doi: 10.1038/nchembio.396

Saturation experiments were performed with [^{125}I]OTA, a mixed vasopressin V_{1a}/oxytocin receptor (OTR) antagonist [12], on membranes from fetal membranes expressing V_{1a} and OT receptors. Membranes (50 µg/assay) were incubated with increasing concentrations of radioactive tracer (20 pM to 1 nM) for 1 h at 30°C. For each concentration of tracer, nonspecific binding was determined by the addition of an excess of OTA (1 µM). Bound and free ligand fractions were separated by filtration as mentioned above.

Data were fitted using the nonlinear curve-fitting routine of the computer software Kell (Biosoft) to the Hill equation : $B = B_{max} [1 + (K_d/[L]^H]^{-1}$, where B_{max} is the maximal binding, [L] is the concentration of labeled ligand, K_d is the equilibrium dissociation constant of the labeled ligand, and H is the Hill coefficient. Of note, fits obtained with a Hill coefficient different of 1 are presented on plots only if they are significantly better (as determined by Kell (Biosoft) software) than those obtained with a Hill coefficient of 1.

For dissociation experiments, membranes (20 µg/assay) from mammary glands were preincubated in a volume of 100 µl for 40 min at 37°C in the presence of [^{3}H]OT (1-2 nM). Three milliliters of incubation medium (50 mM Tris, 5 mM $MgCl_2$, and 1 mg/ml bovine serum albumin) with or without unlabeled OT (1 µM) were then added at different times. The addition of 3 ml of incubation medium dilutes the tracer by a factor of 31. We verified that in such new equilibrium conditions, less than 10% of the binding sites were still able to be labeled by the tracer. At each dissociation time, bound radioactivity was determined as described above. All binding data were analyzed with the program Graphpad Prism using a one phase or two phase exponential decrease.

Nature Chemical Biology: doi: 10.1038/nchembio.396

References

1. Albizu, L. et al. Towards efficient drug screening by homogeneous assays based on the development of new fluorescent vasopressin and oxytocin receptor ligands. *Journal of Medicinal Chemistry* **50**, 4976-85 (2007).
2. Cotte, N. et al. Identification of residues responsible for the selective binding of peptide antagonists and agonists in the V2 vasopressin receptor. *J Biol Chem* **273**, 29462-8 (1998).
3. Chini, B. et al. Two aromatic residues regulate the response of the human oxytocin receptor to the partial agonist arginine vasopressin. *FEBS Lett* **397**, 201-6 (1996).
4. Bazin, H., Preaudat, M., Trinquet, E. & Mathis, G. Homogeneous time resolved fluorescence resonance energy transfer using rare earth cryptates as a tool for probing molecular interactions in biology. *Spectrochim Acta A Mol Biomol Spectrosc* **57**, 2197-211 (2001).
5. Durroux, T. et al. Fluorescent pseudo-peptide linear vasopressin antagonists: design, synthesis, and applications. *J Med Chem* **42**, 1312-9 (1999).
6. Terrillon, S. et al. Synthesis and characterization of fluorescent antagonists and agonists for human oxytocin and vasopressin V(1)(a) receptors. *J Med Chem* **45**, 2579-88 (2002).
7. Manning, M. et al. Synthesis and some pharmacological properties of potent and selective antagonists of the vasopressor (V1-receptor) response to arginine-vasopressin. *J Med Chem* **35**, 382-8 (1992).
8. Bakthavachalam, V., Baindur, N., Madras, B.K. & Neumeyer, J.L. Fluorescent probes for dopamine receptors: synthesis and characterization of fluorescein and 7-nitrobenz-2-oxa-1,3-diazol-4-yl conjugates of D-1 and D-2 receptor ligands. *J Med Chem* **34**, 3235-41 (1991).
9. Cotte, N. et al. Conserved aromatic residues in the transmembrane region VI of the V1a vasopressin receptor differentiate agonist vs. antagonist ligand binding. *Eur J Biochem* **267**, 4253-63 (2000).
10. Elands, J., Barberis, C. & Jard, S. [3H]-[Thr4,Gly7]OT: a highly selective ligand for central and peripheral OT receptors. *Am J Physiol* **254**, E31-8 (1988).
11. Barberis, C. et al. Site-directed mutagenesis of V1a vasopressin receptor: identification of amino-acids involved in ligand binding. in *Vasopressin* (ed. G.L., G.P.R.D.R.) 69-78 (John Libbey Eurotext, 1993).
12. Elands, J. et al. 125I-labelled d(CH2)5[Tyr(Me)2,Thr4,Tyr-NH2(9)]OVT: a selective oxytocin receptor ligand. *Eur J Pharmacol* **147**, 197-207 (1988).

Nature Chemical Biology: doi: 10.1038/nchembio.396